Summer 2022

# Decadal-Scale Effects of Large Wood Restoration on Channel Morphology and Groundwater Connectivity, Taneum Creek, WA

Samuel Fixler
*Central Washington University*, samuel.fixler@cwu.edu

DECADAL-SCALE EFFECTS OF LARGE WOOD RESTORATION ON CHANNEL

MORPHOLOGY AND GROUNDWATER CONNECTIVITY,

TANEUM CREEK, WA

---

A Thesis

Presented to

The Graduate Faculty

Central Washington University

---

In Partial Fulfillment

of the Requirements for the Degree

Master of Science

Geological Sciences

---

by

Samuel A. Fixler

July 2022

CENTRAL WASHINGTON UNIVERSITY

Graduate Studies

We hereby approve the thesis of

Samuel A. Fixler

Candidate for the degree of Master of Science

APPROVED FOR THE GRADUATE FACULTY

Dr. Lisa Ely, Committee Chair

Dr. Carey Gazis

Dr. Jennifer Lipton

Dean of Graduate Studies

ABSTRACT

DECADAL-SCALE EFFECTS OF LARGE WOOD RESTORATION ON CHANNEL MORPHOLOGY AND GROUNDWATER CONNECTIVITY, TANEUM CREEK, WA

by Samuel A. Fixler

July, 2022

The importance of large wood (LW) in creating channel complexity is widely recognized; however, few LW projects have been in place long enough to track meaningful channel changes on a decadal timescale. Taneum Creek, located in central Washington, is one of the earliest LW restoration areas (2008) in the Yakima River Basin and the central Cascade Mountains. The flood in 2011, with an estimated discharge of 69 $m^3/s$ (2,400-2,800 cfs), provided further channel change by mobilizing LW and channel sediments. Three reaches with similar channel characteristics and LW additions were compared with a control reach without LW additions to document this annual channel change. The effect of LW on annual floodplain connectivity was further assessed using a normalized difference vegetation index (NDVI), which represents density of greenness and plant health. This index is used as a proxy for floodplain ‘greenness’, which will help illustrate floodplain connectivity.

In response to the large flood of 2011, LW created new channel complexity, such as significant increases in multi-threaded channels in each of the LW study reaches, except the control reach, as well as side-channel formation which allowed for beaver dam construction. Of the side channels that formed in the LW reaches, 50% or more formed 10 m downstream of LW jams. Sinuosity increases were not uniform among the different reaches with fluctuating increases and decreases. The reaches with increased channel complexity related to the LW and large flood also increased in floodplain greenness and connectivity. This increase is likely a result of the floodplain inundation that increased delivery of water to side channels and beaver ponds and perhaps raising the local groundwater table. The results of the study indicate that the reaches with LW additions increased in channel complexity and groundwater-floodplain connectivity following the large flood, which is important for maintaining diverse aquatic and riparian species and possible aquifer recharge.

## ACKNOWLEDGEMENTS

This research was partially funded by the Washington Section of the American Water Resources Association (AWRA) and the Central Washington University (CWU) Graduate Student Summer Fellowship. I would like to thank these two organizations for allowing me to dedicate the summer of 2021 to this research. My fieldwork was made possible with the help of my wonderful field assistants: Justin Nickolaus, Dawson Miller, and Abbey Crowe. I would also like to thank Emil Babik and fellow master’s students Edward Vlasenko, Bethany Kharrazi, Emily Polizzi and Catherine Jones for helping with the drone flights and fieldwork. I would like to thank Dr. Carey Gazis and Dr. Jennifer Lipton for their help with fieldwork and remote sensing. I would like to thank Dr. Lisa Ely, my advisor and mentor for her constant support throughout this process. Finally, I would like to thank my parents, Claude Fixler and Lynn Whitney for their encouragement and support.

TABLE OF CONTENTS

TABLE OF CONTENTS (CONTINUED)

LIST OF TABLES

LIST OF FIGURES

LIST OF FIGURES (CONTINUED)

Figure Page

# CHAPTER I

# INTRODUCTION

## A Brief History of Large Wood

Large wood additions in streams are one of the most common restoration tools. As early as the 1890s, landowners in the eastern US began placing wood in channels to improve fish habitat (Thompson and Stull, 2002). The success of LW in streams in the eastern US resulted in the addition of LW as a restoration tool in the Pacific Northwest (PNW) (Abbe and Montgomery, 1996; Nagayama and Nakamura, 2010) However, because PNW streams have generally steep gradients and higher stream power, restoration transitioned to adding LW jams instead of single LW pieces (Roni et al., 2015). Over time, restoration practices evolved to include LW root wads, which help stabilize LW in the streams and floodplains (Abbe and Montgomery, 1996; Collins and Montgomery, 2002; Roni et al., 2015; Collins et al., 2012). However, in larger river systems, engineered structures are still used for safety and liability reasons (Roni et al., 2015; Abbe and Brooks, 2011).

The streams in the PNW have been subject to anthropogenically influenced alterations since the beginning of colonial settlement. In a natural setting, wood would be recruited by the stream through several processes: tree fall, debris flows, landslides, and erosion (Abbe and Montgomery, 1996; Collins and Montgomery, 2002; Collins et al., 2012; Roni et al., 2015; Comiti et al., 2016; Martin et al., 2021; Swanson et al, 2021). However, logging and log drives of wood near channels has significantly reduced the amount of LW in the river systems of the PNW. The high gradient streams would generally have a large amount of LW in the natural system, but the lack of LW and the proven correlation between LW and fish habitat, has resulted in the addition of LW as a restoration technique, starting in the 1990s (Roni et al., 2015; Grabowski et al., 2019).

## Project Purpose

The purpose of this research is to determine the long-term effects of large wood restoration on channel patterns, floodplain connectivity, and groundwater-surface water interaction. Taneum Creek, in central Washington, provides an ideal study site to address these questions. The watershed experienced channel wood restoration in 2008-2010 followed by a large flood in 2011 that mobilized the large wood (LW) and channel sediment. The relationship between channel change and LW was examined by calculating sinuosity and multithreaded indices at locations with and without LW. The dynamics of LW and floodplain connectivity was investigated using NDVI (Normalized Difference Vegetation Index) analysis as a proxy for floodplain "greenness". Groundwater-surface water interaction was indicated by salinity, temperature, upwelling and downwelling near LW sites.

## Description of Taneum Creek

Taneum Creek is a tributary of the Yakima River located in Kittitas County, WA, approximately 17 km northwest of Ellensburg (Figure 1). Taneum Creek flows from west to east from its North and South forks and joins the Yakima River at river mile 166.1 (Monk, 2009). The total basin area is approximately 215 km$^2$ (Jones and Stokes, 1991). Precipitation ranges from over 150 cm in the upper basin, to 25 cm near the confluence with the Yakima River (Monk, 2009). Elevations range from 1914 m at Quartz Mountain to 515 m at the confluence with the Yakima River (Toth, 1995; Jones and Stokes, 1991) Taneum Creek has been identified as suitable habitat for supporting steelhead trout (Oncorhynchus mykiss) and salmon (Monk, 2015). Restoration on Taneum Creek has included removing dams and irrigation screening diversions, building fish passage, and adding LW (Monk, 2015). The fish passageway constructed in the late 1980s and 1990s opened up miles of stream habitat for trout and salmon (Monk, 2015). The Brunton Diversion dam was removed when steelhead were considered endangered in the Yakima Basin in 1999, and the channel surrounding the dam was restored to a healthier state (Monk, 2015).

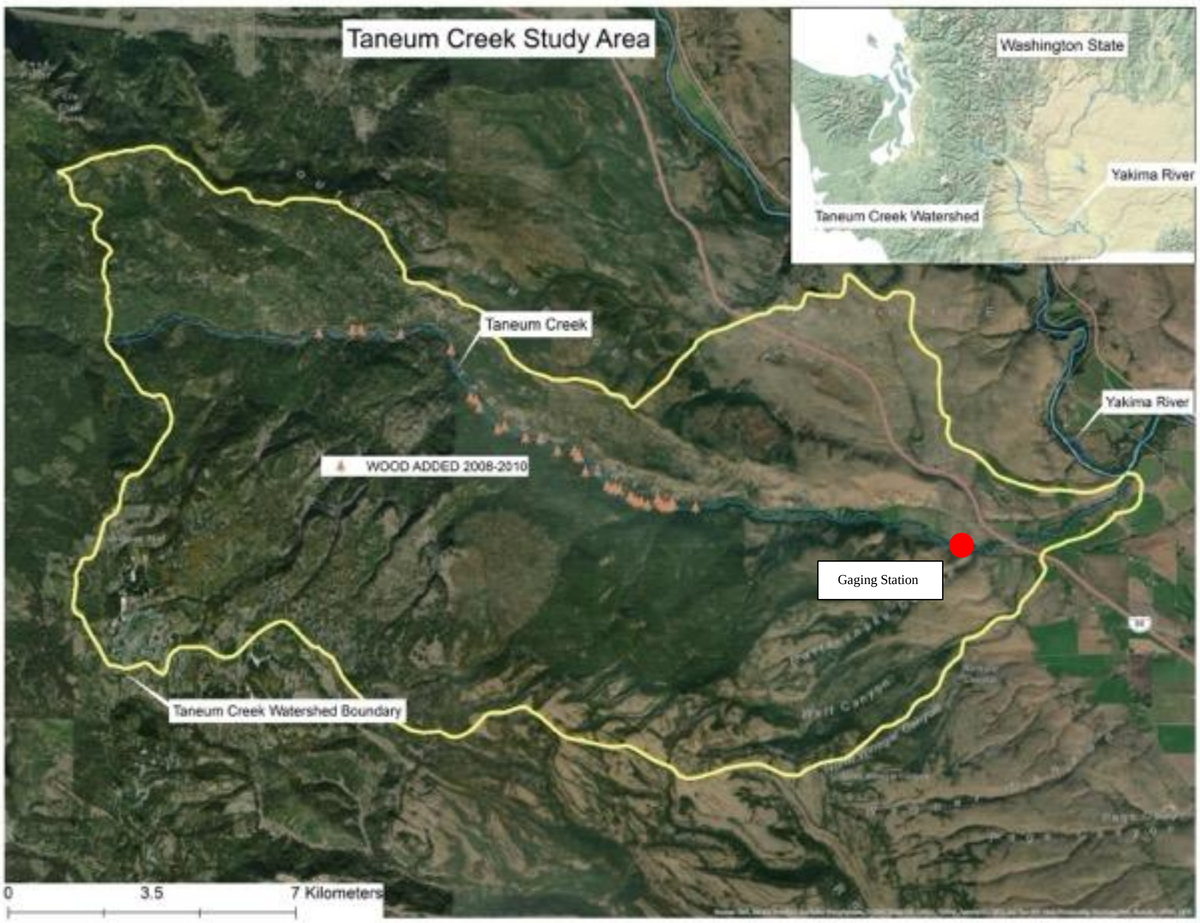


Figure 1: The Taneum Creek study area located in central Washington. The locations of the LW are shown with brown triangles, with over 200 pieces placed since 2008. The Brain Ranch gaging station is located south of Interstate 90, upstream of the irrigation diversion canal.

The Washington Department of Fish and Wildlife (WDFW), Kittitas Reclamation District, Yakama Nation Fisheries, Washington Water Trust, Kittitas Conservation Trust, Taneum Canal Company, and local landowners partnered together to restore salmon and steelhead habitat in the creek (Monk, 2015). The restoration involved increasing summer stream flow, adding hundreds of LW jams, and restoration fish passage barriers (Monk, 2015) With this collaboration, LW additions became a critical piece in restoring habitat for these anadromous fish species. The restoration practices conducted in Taneum Creek has resulted in a positive impact for returning fish species (Monk, 2015).

## Yakima Basin Integrated Plan

The Yakima Basin Integrated plan was created to address hydrological issues facing central Washington in the Yakima Basin (YBIP). It is expected that the snowpack of the Cascades will decrease (Gergel et al., 2017), on which the Yakima Basin and its various users rely. The creation of YBIP is designed to address these future water issues by focusing on these seven elements: reservoir fish passage, structural and operational changes, surface water storage, groundwater storage, habitat/watershed protection, enhanced water conservation, and market reallocation.

## Large Wood and Fish Species

Large Wood is now used as a common restoration tool used to create pools, create cover, trap sediments, and modify other channel geometries for the creation of habitat for trout and salmon, especially relevant to Taneum Creek. The important relationship between LW and salmon was researched as early as the 1970s (Beechie et al., 2013; Jones et al., 2014; Roni et al., 2015; Gonzalez et al., 2017). In smaller streams of the PNW, LW has been shown to produce several positive effects. LW can entrain and store sediments, form pools, retain organic matter, decrease bed grain size, and partially convert bedrock channels to alluvial channels (Abbe and Montgomery, 1996; Buffington and Montgomery, 1999; Roni et al., 2015). LW is important for spawning salmonids by controlling bed sediment sizes and by creating pools (Dolloff et al., 2003; Roni et al., 2015). The connection between LW and improving fish habitat is one of the main factors that LW is used in stream restoration. It has been documented that salmon and trout species have a significant positive response to LW additions in streams, like log jams, or channel spanning LW (Whiteway et al. 2010). Whiteway et al. (2010) used data from over 211 streams in 51 different studies to reach this conclusion. They examined salmonid response to wood and other structure placement using data from 211 streams from 51 different studies and found significant improvements in physical habitat and positive and significant responses for most species of salmonid fishes (Figure 1; Roni et al., 2015; Whiteway et al., 2010).

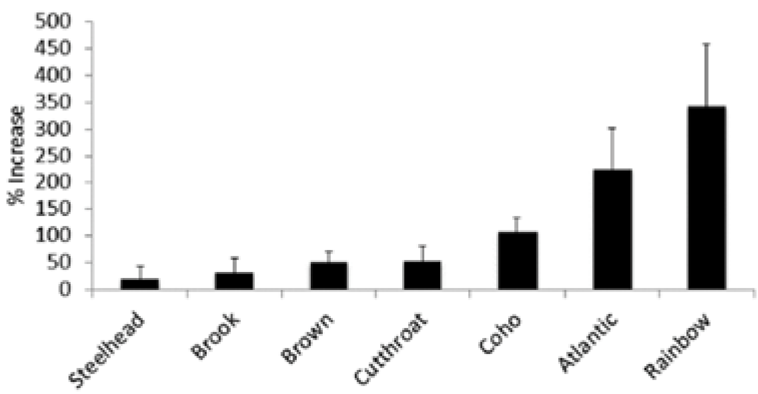


Figure 2: Response of trout and salmon species to LW addition projects. Adapted from Roni et al., 2015 and Whiteway et al., 2010.

## Hydraulics of Large Wood

Large wood additions in rivers traps fine sediments as velocity is reduced closer to large wood (May and Gresswell, 2003; Osei et al., 2015). Large wood can trap fines and organic matter, which can increases geomorphic and habitat complexity. Large wood can also scour out pools because it traps fines from entering them, which is important for fish habitat during low flows (Martin, 2001). The ability of LW to trap fines is important because it can remove fines from important spawning gravels for salmon and trout. Decreased fine sediment in gravels and cobbles is important for survivability of these spawning redds.

In NW Washington, a study investigating the relationships between channel characteristics and LW found that there is a relationship between LW and pool area or spacing in NW Washington State (Beechie and Sibley, 1997). The authors suggest that low gradient streams are less influenced by LW additions, and that LW has a greater effect on channels with a moderate gradient (Beechie and Sibley, 1997; Figure 3). The regression models used by the authors showed that the influence of LW changes with slope. The size of the LW jams that formed pools also increases with increases in channel width (Fetherston et al., 1995; Beechie and Sibley, 1997; Abbe and Montgomery, 2002). In low gradient streams, pools are formed by other mechanisms than LW. Therefore, because Taneum Creek is a mountain stream, LW would be considered a driving factor in channel geometry. Large wood also influences sediment characteristics of a channel. Multiple studies have examined the effect of LW on sediment sorting and LW's ability to be initial vegetation sites (Abbe and Montgomery, 1996; Collins et al., 2012). Large wood traps fines, which allow vegetation to colonize increasing banks stability (Collins et al., 2012), which would increase floodplain greenness.

Large wood plays a key role in floodplain development; LW is the primary driver of channel morphology in many mountain streams in the PNW because it forms pools, regulates sediment transport, creates waterfalls, and provides habitat for fish and other aquatic life (Fetherston et al., 1995). LW in the channel, or in a floodplain can create low velocity area, where sediment can deposit, creating locations for formation of vegetation over time (Fetherston et al., 1995). In these small channels, LW can store a large portion of sediment in the channel, up to 47% in small streams in Idaho (Megahan, 1982; Fetherston et al., 1995). The removal of LW can result in catastrophic releases of sediment. LW was removed from a reach in an Oregon stream, releasing 5250 $m^3$of sediment (Beschta, 1979; Fetherston et al., 1995). Based on the available literature, LW is extremely important in controlling sediment fluxes in mountain streams.

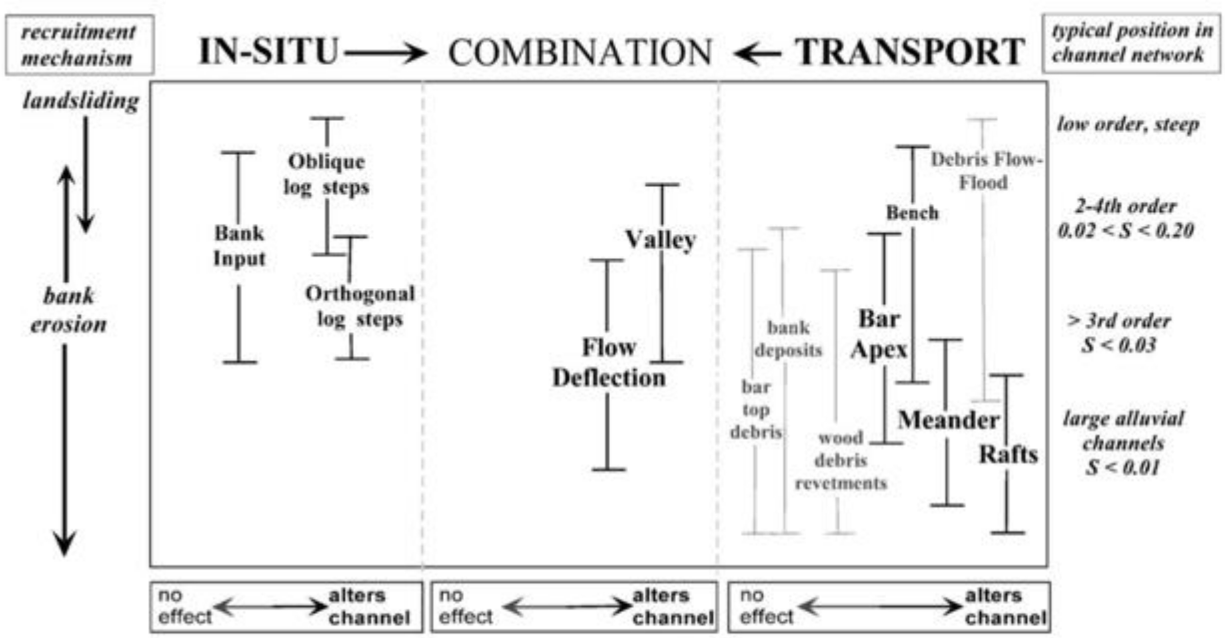


Figure 3: LW accumulation types and their position in a drainage network (Abbe and Montgomery, 2002).

Large wood plays a role in creating sediment stocks when placed on floodplains. Large wood creates alluvial areas of erosion-resistant material that can be quickly stabilized by vegetation (Collins et al., 2012). In frequently flooded areas, fine alluvial deposits accumulate through mechanical action from trees, potentially impacting forest regeneration (Hümann et al., 2011; Saint-Laurent et al., 2019:). In riparian forest stands LW deposition increases as they are pinned to standing trees, providing nutrients to the soil (Collins et al., 2012; Lininger et al., 2019; Lininger et al., 2021). The LW pinned to floodplains increases nitrate and phosphate uptake in the soil, correlating to the volume and frequency of the jams (Collins et al., 2012). In-channel LW also accumulates organic carbons stocks in the backwater being the LW jams, increasing carbon storage of streambank soils (Collins et al., 2012).

## Large Wood and Flooding

Fluvial systems in different ecological areas can respond differently to catastrophic floods. The response of LW is highly dependent on catchment variability, resulting in little consensus on the geomorphic effects of large floods on different stream types and locales (Roni et al., 2015; Comiti et al., 2016) Large floods have been shown to widen and erode rivers, however large floods can entrain, transport, and deposit coarse bed material (Magilligan et al.,2014). Large floods can strip the floodplain and deposit coarse bed material across it (Magilligan et al., 2014). In mountain streams, channel widening occurs in most of the channels, and those major geomorphological changes occurred after the flood peak (Surian et al., 2016). The major factor controlling channel response to flood events is the calculated unit stream power suggesting that width increases could increase after the peak flood (Surian et al., 2016). Large floods can be the dominant geomorphological modifier in mountain streams, making them an extensively studied aspect in fluvial geomorphology.

The dynamics between LW and flooding detailed in Figure 4, illustrates how LW accumulates based on drainage size. It illustrates that small mountain streams are heavily controlled by LW and their response to flooding. During a large flood, LW typically causes obstructions at constrictions or structures in a channel, like bridges or weirs (Comiti et al., 2016). High-magnitude events and the response of LW is generally catchment specific, especially in the recruitment phase for LW (floodplain or hillslope) (Figure 4; Comiti et al. 2016). The extent of LW recruitment in mountain streams also relies heavily on the connectivity of the floodplain or hillslope to the channel (Fetherson et al, 1995; Comiti et al., 2016). Figure 4, obtained by Comiti et al. (2016), details how LW accumulates in a stream, illustrating how small mountain streams rely on hillslopes and floodplains for recruitment. Transport of LW in a large flood is supply-limited, and deposition of LW is mostly observed at man-made structures (Comiti et al., 2016). This is especially important for fluvial systems like Taneum Creek, where the large flood in 2011 caused significant geomorphological changes.

## Groundwater

The interactions of stream channel restoration with floodplain or channel LW and groundwater is relatively understudied. Recent studies suggest no interaction between groundwater levels and floodplain LW in central Washington (Bartlett, 2022), however others suggest there might be some increased storage (Boylan, 2019). However, in Trout Creek, California the effects of channel restoration and floodplain restoration resulted in a positive

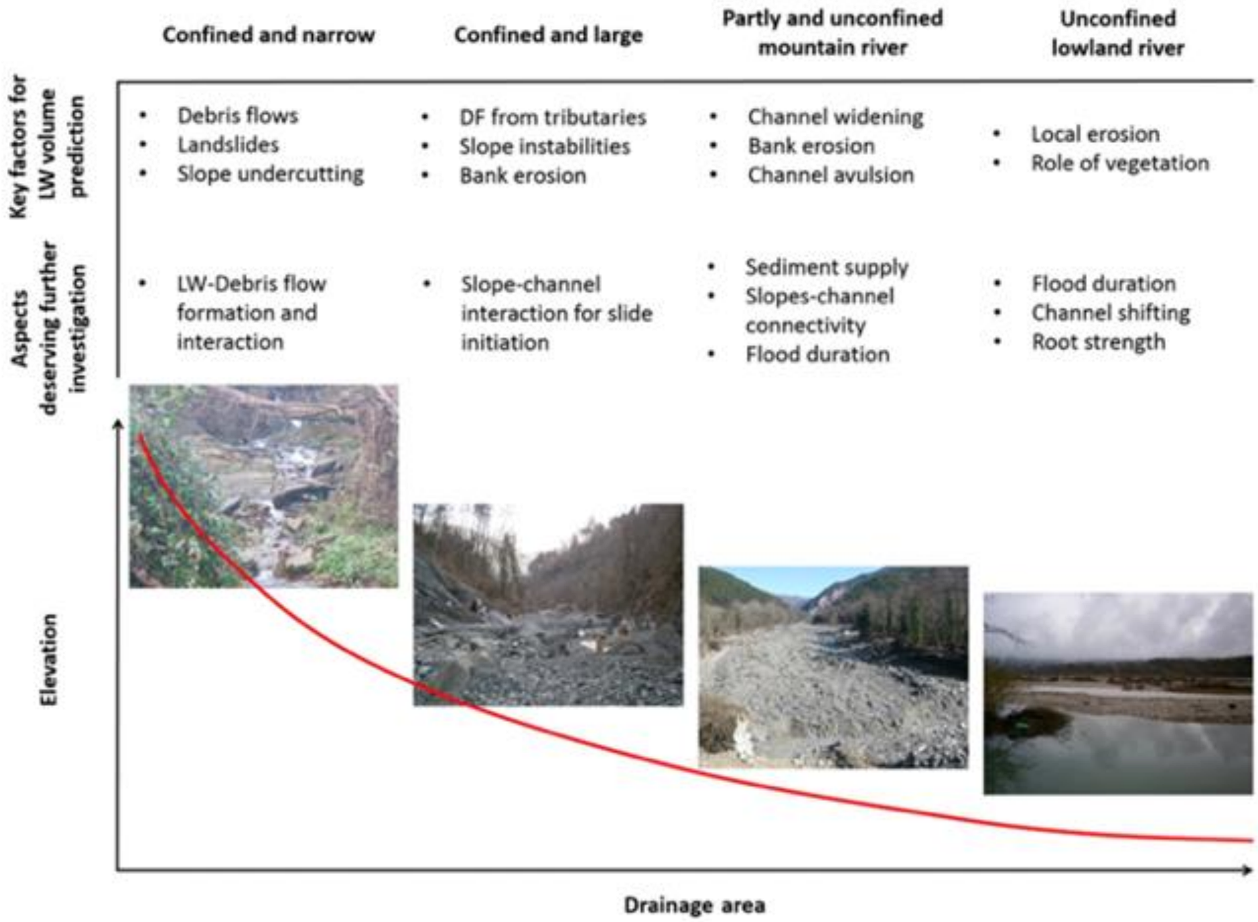


Figure 4: Prediction of LW transport in different channel types from Comiti et al. (2016). Elevation and drainage area are key factors in LW recruitment in different catchments. "DF" indicates debris flow. The entire watershed of Taneum Creek would fulfill all properties except 'unconfined lowland river'.

seasonal impact on streamflow during the summer and decreased groundwater table depths (Tague et al., 2008).

In a study investigating the groundwater of the upper Yakima River basin by Gendaszek et al. (2014), the authors suggest that general groundwater movement is towards the Yakima River in the unconfined aquifers in the unconsolidated sediments. Groundwater movement through the aquifers of the Yakima River basin is complex, with distinct aquifer systems (Gendaszek et al., 2014). Groundwater recharge in one subbasin is not available for withdrawal or discharge into surface-water features in other subbasins (Gendaszek et al., 2014). In the basin, cool groundwater inflow is only in discrete sections of stream tributaries of the Yakima River, and the authors suggest that there is evidence for continuity between groundwater and surface water systems (Gendaszek et al., 2014). This is important for restoration in the Yakima River basin because restoring groundwater is a central theme of the Yakima Basin Integrated Plan (YBIP). The connection between groundwater and surface water in LW restoration sites is one component of this system.

Large wood interacts with fluvial systems in a variety of ways. Recruitment of LW into a stream system is not only especially important for aquatic habitat, but for the overall geomorphological function of mountain streams. The movement of LW in a system is controlled by the morphology of the stream. There are still many aspects of the interactions between LW and groundwater to be explored like how groundwater storage interacts with LW on floodplains. The Yakima River basin is the ideal environment for such a study, and the complexity of Taneum Creek makes it an ideal study area for the research of LW, groundwater, and channel change.

## Study Area

Four reaches were chosen in the lower watershed of Taneum Creek to investigate the extent of channel changes related to the large flood of 2011, LW additions, floodplain greenness, and groundwater surface water interactions at LW sites. Each reach was selected for its unique characteristics in suspected channel change (Figure 5).

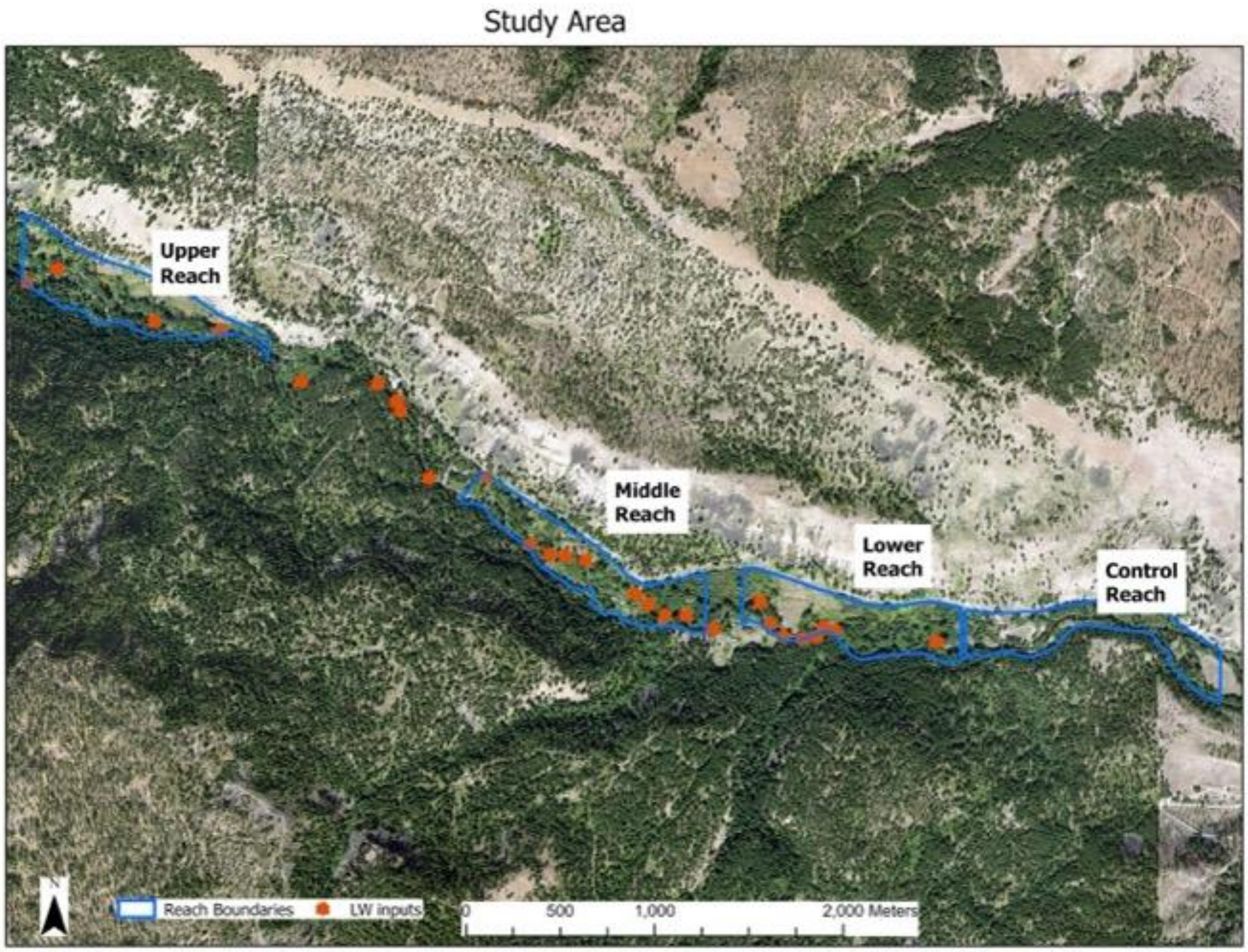


Figure 5: The study areas for the three LW reaches and the control reach. The valley lengths for each multi-threaded channel index and sinuosity index are marked. The locations and numbers of large wood are marked for each reach boundary. Salinity and temperature cross-sections were taken at small subsets near large wood jams for each study reach. (Figure 6).

All four reaches were selected for their similar characteristics in channel morphology, bed structure, and floodplain valley width extent. The upper reach, middle reach, and lower reach all received LW additions in 2008, while the control reach did not. The lower reach was selected for its unique characteristics, potentially formed by the large flood and LW additions, like the side channel cutting through the floodplain (Nicolai, personal communication, 2020; Figure 5). The middle reach was selected for its multi-threaded channels that potentially formed during the large flood of 2011 (Nicolai, personal communication, 2020; Figure 5). The upper reach was also selected for its unique increases in channel sinuosity and threading and floodplain connectivity increases that potentially occurred as a result of the LW and large flood of 2011 (Nicolai, personal communication, 2020; Figure 5).

## Beaver Impacts on Floodplains

Beavers select dam sites based on a set of complex characteristics from vegetation to substrate. A study in Eastern Oregon concluded that beavers build dams in shallow lower gradient reaches and not on rock substrates (McComb et al., 1995). Tree cover of occupied beaver dam reaches was greater than unoccupied sites, specifically in alder abundance (McComb et al., 1995). Based on these studies, it appears that beavers will occupy the main stem on smaller low gradient streams compared to occupying channels in larger streams.

Beaver dam meadows impact the soils by creating carbon sinks. In beaver meadows, carbon density was significantly greater than in adjacent unoccupied forest floodplain (Johnston, 2014). The soils of beaver meadows generally have a thick O horizon with significant carbon storage, that is unaffected by parent material origin (Johnston, 2014).

Beaver dam location, spatial orientation, and pond sequences also change the textures of the soils in the ponds. Generally coarse material is deposited at the upstream and downstream ends of the ponds, and fine material is deposited in the middle (Butler and Malanson, 1995; Bigler et al., 2001). This data generally correlates to the higher velocities found at the ends of the dams and lower velocities in the middle.

Beaver dams and meadows alter floodplain organic carbon storage regimes. In a study within the Front Range of Colorado examining soil moisture, soil depth, percent clay content, organic carbon concentration to compare beaver meadows, Laurel and Wohl (2018) found that mean soil moisture only differs between active and old abandoned meadows. The authors also found that soil depth and organic carbon stock do not differ between beaver meadows, indicating parent material controls which regenerate and maintain organic carbon, even after meadow abandonment (Laurel and Wohl, 2018). Early studies suggest that organic carbon storage in floodplain meadows can persist for decades (Laurel and Wohl, 2018; Johnston, 2014).

# CHAPTER II

# BACKGROUND

## Large Flood of 2011

Taneum Creek experienced an exceptionally large flood in 2011 that likely created new channel characteristics to be examined in this study (Figure 6; Figure 7). The discharge of the large flood that occurred at Taneum Creek on May 15, 2011, was estimated by Paul Tappel, using a rating curve and flow measurements taken during the large flood. Tappel (2012) estimated the discharge to be 69 -79 $m^3/s$ (2,400 to 2,800 cfs). As noted in the report, Tappel (2012) stated that the measurements were produced without the stringent standards used by the USGS, however the confidence in the discharge range was high. The discharge estimate was approximately 11 - 23 $m^3/s$ (400-800 cfs) above the 100-year flood of 57$m^3/s$ (2,000 cfs) (Tappel, 2012). Most of the logs placed by the Yakama Nation moved to create large log jams but did not move far enough downstream to impact downstream landowners (Tappel, 2012; Figure 8).

Figure 6: The large flood of May 15, 2011, near the intake to the Taneum irrigation canal. Photo taken by Paul Tappel, 2011.

Figure 7: The large flood of May 15, 2011, near the access bridge to the Taneum irrigation canal. Photo taken by Paul Tappel, 2011.

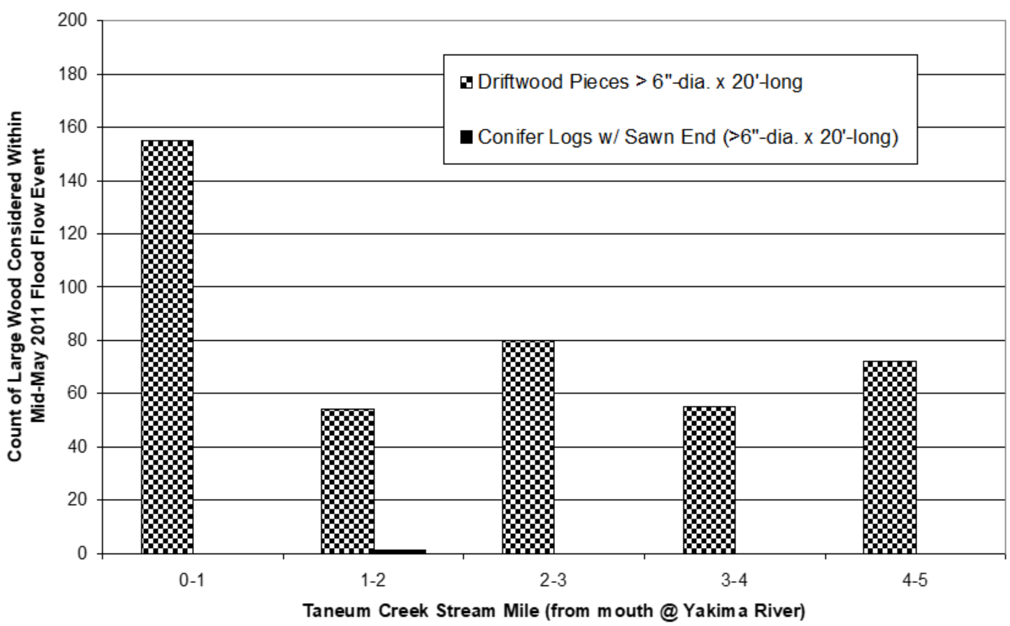


Figure 8: The LW count completed by Tappel (2012) on downstream landowner property. A total of 417 logs were counted and only a few LW restoration pieces moved far enough downstream onto private property (from Tappel, 2012).

## Geology of Lower Taneum Creek

Lower Taneum Creek consists mostly of Quaternary alluvium. The surface geology of valley width consists of unconsolidated or semi-consolidated alluvial clay, silt, sand, gravel, and (or) cobble deposit (Lewellen et al., 1985). Local surface geology of the area includes peat, muck, and diatomite, marsh, landslide, lahar, glacial, colluvial deposits, volcaniclastic or tephra deposits, and artificial fill (Lewellen et al., 1985).

Southern and northern valley slopes contain mostly landslide deposits, talus, colluvium, protalus ramparts, rock glaciers; and 1980 ash from Mount St. Helens (Lewellen et al., 1985). Southern and northern valley walls consist mostly of Miocene fine-grained flood basalt flows (Lewellen et al., 1985). Valley walls also consist of flood basalt sills and dikes, hyaloclastite, pillowed lava flows, and peperites (Lewellen et al., 1985). Intercanyon consist of, saprolites, and pillow-palagonite complexes (Lewellen et al., 1985). Plagioclase-phyric flood basalt in the canyon is commonly interbedded with tuffaceous sandstone, siltstone, and conglomerate, most of which are parts of the Ellensburg and Latah Formations (Lewellen et al., 1985).

## Hydrogeology of Taneum Creek

Taneum Creek watershed is a relatively simple hydrogeological area, where groundwater and surface water interact to form habitat for a variety of fish species. Taneum Creek relies on a combination of groundwater and surface water to maintain flows; however, during the summer months much of the discharge is a result of groundwater baseflow (Monk, 2009). Understanding how the groundwater interacts with the creek is critical for multiple reasons, ranging from habitat to agricultural uses.

Taneum Creek watershed consists of two distinct bedrock hydrologeologic units, the Columbia River Basalt Group (CRBG) and older bedrock (Vaccaro et al. 2009). The alluvial floodplain aquifer might be maintained by these units or the sedimentary layers like the Ellensburg formation (Vaccaro et al. 2009). Taneum creek is mostly underlain by basalt There are some units of quaternary fill and sedimentary formations (Vaccaro et al. 2009; Figure 9). These underlying basalts likely form the groundwater system that supplies Taneum Creek (Figure 10).

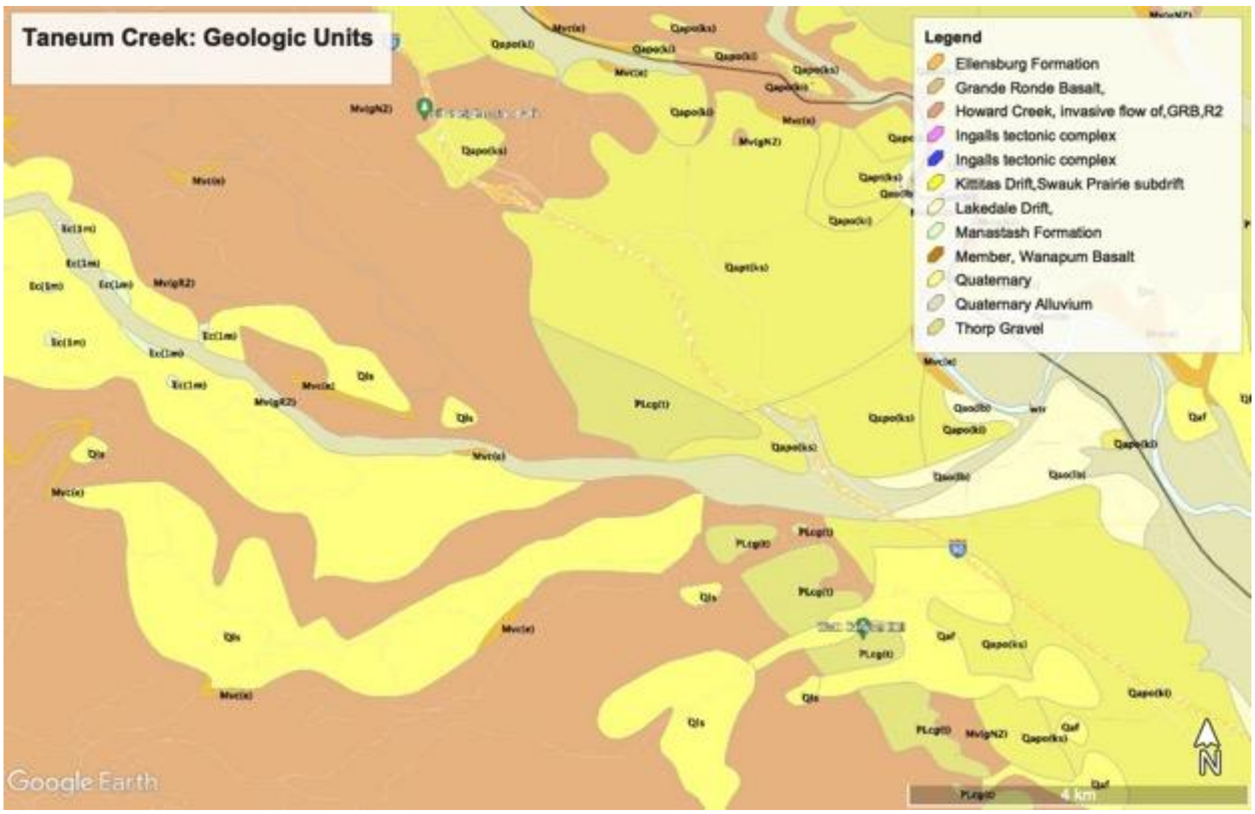


Figure 9: The geologic units of Taneum Creek (WA DNR) (Tabor et al., 1982).

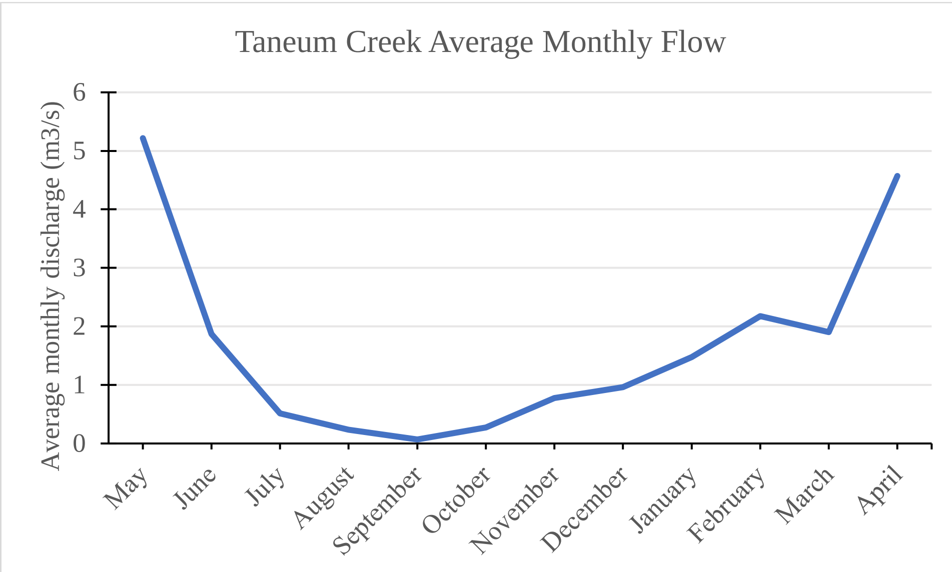


Figure 10: Average monthly flow ($m^3/s$) for Taneum Creek at the Brain Ranch gage from May 2005 – October 2020. Data was collected from WA Department of Ecology Station 39P080. Peak discharge is generally in late May, with groundwater base flow dominating in July (Monk, 2009).

The groundwater of Taneum Creek moves through several underlying basalt layers. The groundwater of Taneum Creek basin moves through the fracture systems of the Paleozoic metamorphic rocks in the upper portion of the Taneum Creek basin (Ely et al., 2011: Gendaszek et al., 2014). The lower portion of the basin is dominated by the Columbia River Basalt Group and its associated groundwater regime (Vacarro et al., 2009). Other units include floodplain alluvial deposits, unconsolidated loess, alluvial fan, and (Vacarro et al., 2009). These deposits also form their own unique aquifer system (Ely et al., 2011; Vaccaro et a., 2009) These geologic structures combine to create an aquifer system in the Taneum Creek basin. Taneum Creek relies on groundwater in the summer months to maintain baseflow, highlighting the importance for the understanding of the groundwater regime.

# CHAPTER III

# METHODS

The methods designed to achieve the objectives for this project involve a combination of remote sensing techniques, field work, and GIS analysis. Channel sinuosity and multithread braiding indices, salinity; temperature and piezometer groundwater analysis; and NDVI calculations were used to develop a picture of LW impacts on Taneum Creek.

## Channel Sinuosity and Multi-threaded Channel Index

The main channels and active side channels of Taneum Creek were digitized on ArcPro using imagery from the NAIP (National Agriculture Imagery Program) database, which is aerial imagery developed by the U.S. Department of Agriculture (USDA). The imagery has been collected during agricultural growing seasons since 2003 (NAIP, 2013). The imagery for this project was collected on the dates: 7/16/06, 7/1/09, 8/18/11, 8/18/13, 7/30/15, 10/9/17, and 10/14/19. For the purposes of simplicity this will be considered 2006 to 2019. The channels were digitized to quantify changes in channel sinuosity and braiding over time. The main channel was defined as the widest active channel, while other active channels were considered side channels. Only side channels that avulsed and reconnected to the main channel were mapped. Sinuosity values for the main channel were calculated for each study reach by measuring the length of the main channel and dividing the length by the straight-line distance of the river valley in each defined reach (Hong and Davies 1979 and Equation 1). Channel sinuosity lines were digitized in the center of the main channel. The same process was repeated for each aerial imagery year, which occurred in late summer, for a total of 42 sinuosity values.

Equation (1) Sinuosity = Main Channel Length (m) / Straight valley distance (m)

Channel braiding or multi-threaded channel index (MTCI) calculations were calculated using the cumulative channel length method, similar to the methodology of Hong and Davies (1979) and Friend and Sinha (1993). Side channels were identified as any channel smaller in width than the main channel. Side channels created by beaver ponds were measured in straight line distance to their outlet into the main channel. Cumulative side channel lengths were divided by same straight-line valley length of each reach to yield a MTCI index value (Equation 2). This process was repeated for each aerial imagery year for a total of 42 values

Equation (2) Sinuosity = Cumulative Side Channel Length (m) / Straight valley distance (m)

The drone imagery for the three LW reaches was used to determine proximity of side channels LW jams. The drone imagery was used instead of the NDVI imagery because the coarse resolution did represent all LW jams. The LW jams were buffered 10m and compared to the delineated MTCI channels. If a side channel was present downstream and within the buffer for the years after the large flood of 2011, then LW was considered a driving factor in the channel avulsion.

## Piezometer Analysis

To measure groundwater and surface flow interaction in the hyporheic zone, a 100-cm long piezometer (Figure 14) was used along the three reaches along Taneum Creek. The piezometer was pounded into the substrate using a post pounder to at least the depth of the slotted holes. The exact locations varied depending on substrate conditions, but piezometers were installed upstream, downstream, and at LW locations at all study reaches with the target goal of at least 5 installations. Locations were marked with GPS and sediment grain size was recorded. Locations of the measurements depended heavily on bed type and did not remain consistent in relation to LW at the three study reaches. When installing the piezometer, the best available location for driving the post in was chosen, which did not always fit a cross section. However, when possible the piezometer was installed on the cross-section in the thalweg of the stream. One minute was allowed to pass for pressure to equalize in the piezometer. The sediment size was not fine enough to clog the piezometer holes, so no developing was required. The water height (inside and outside) the piezometer was recorded (cm), and piezometer height (inside and outside) above bed was recorded (cm) using a meter stick. The water heights (inside and outside) were subtracted from the respective top to bed values (inside and outside) to determine upwelling, downwelling, or equal groundwater pressure. Ten measurements were conducted at the lower reach: eleven at the middle reach, and eight at the upper reach.


Figure 11: Left- The piezometer, which is 1m in length. The slotted ends were driven into the bed substrate as far as possible. Right- The piezometer at the middle reach, downstream of a LW log jam.

## NDVI Analysis

To measure floodplain greenness, Level 2, Landsat 5 and 8 imageries were collected from 2006 to 2020 during the month of August for the Taneum Creek study areas. Care was taken to collect cloud free imagery within the study area. The spatial resolution of the bands is 30 m. All NDVI analysis was completed in ArcPro. The Landsat images were clipped to the Taneum Creek reach boundaries and bands were separated with the NDVI tool in ArcPro and converted into NDVI imagery to represent ‘greenness values’ throughout the study area over the past 14 years. (Equation 3). The rasters were then geoprocessed to a time series to show differences in greenness over time. The greenness is a proxy for floodplain connectivity (Wigmore et al., 2014), which can represent wetting of the floodplain and subsequent vegetation growth/photosynthesis production through side channel inundation, beaver ponds, and groundwater connectivity.

Equation (2) NDVI = (NIR – Red) / (NIR + Red)

## Conductivity Groundwater Cross-sections

To analyze groundwater upwelling, salinity and temperature cross-sections were conducted at the three study reaches using a Thermo Scientific conductivity meter, a 50m tape, and a meter stick. Cross sections for the upper and middle reaches were conducted every 5m along transects that extended 25m above and below LW jams for a total of 10 cross sections. Cross sections in the lower reach were conducted in a section with the most LW jams. The 25m longitudinal distance of each cross section was placed at the center of the log jam. Transects were set up every 5m at the upstream and downstream of the selected LW jam for 50m. However, in the lower reach, not all transects could be completed because the LW was too close together and too large to take equal measurements. Cross-sections started at bankfull width on the right bank (RB) to bankfull width on the left bank (LB). The endpoints of each cross-section were recorded in a GPS. Measurements were taken every 0.5m unless there was an obstruction, in which case the measurement would be taken at the closest active channel point along the transect. Water depths (cm) and bed type measurements were taken at each transect point where the conductivity meter measurements were conducted. Temperature ($^0$C) and Salinity (um) measurements were recorded once the conductivity meter reached equilibrium.

Figure 12: Justin Nichols conducting a cross-sectional survey in the lower reach. Photo is facing upstream.

To establish a reach-wide profile of groundwater-surface water interaction, a methodology was established similar to the thermal profiling of Vaccaro and Maloy (2006). Areas of upwelling tend to have a higher ambient conductivity than areas without upwelling (Vaccaro and Maloy, 2006) A conductivity probe was tied into a 1 m x 5 cm PVC tube with slotted holes. Measurements were taken with the probe every 1 second and tied to GPS tracks. The measurements began at the downstream end of each reach, with the tube and probe dragged behind the user as close to the streambed as possible. Notes were taken at GPS waypoints to designate obstructions or if the probe was taken out of the water. The data was filtered to ignore data above average water temperature when the probe was removed from the creek by timing GPS tracks to the conductivity probe measurements.

## Statistical Tests

A Mann-Whitney U 1 tailed greater than test was run using R statistical software to compare sinuosity, MTCI, and NDVI values for the control and LW reaches before and after the large flood (McKnight and Najab, 2010; R Core Team, 2020). This test was used because the data is non-parametric and is used to determine a difference between dependent variables for two independent groups (McKnight and Najab, 2010). The averages for the LW reaches were compared from 2006-2010 to the 2011-2019 years (excluding 2012) for NDVI data. The averages for sinuosity and MTCI were compared from the 2006 and 2009 data to the 2011, 2013, 2015, and 2019 data.

## CHAPTER IV

## RESULTS

The four study reaches of Taneum Creek showed channel change for all three LW reaches. The middle and upper LW reaches were the only reaches were successful cross-sections could be analyzed. Some data for the lower reach and upper reach was inconclusive. The sinuosity and MTCI indices for all four reaches present a comprehensive picture of channel change over the past decade (Figure 13).

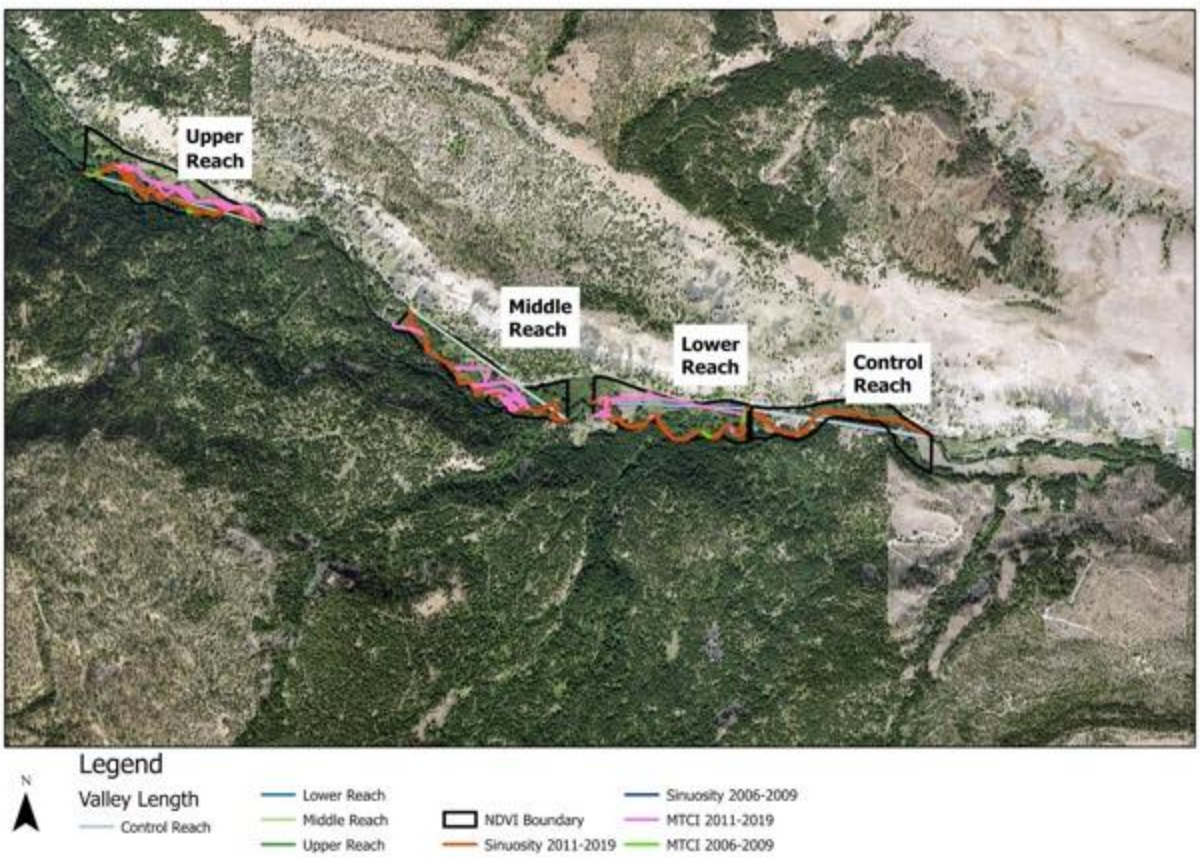


Figure 13: The three study reaches and the control reach. MTCI and sinuosity indices in this figure are combined to represent the channel before and after the large flood of 2011. The valley lengths and NDVI boundaries outline the study area extents for each reach.

## Sinuosity

Changes in sinuosity varied for each reach. The lower reach saw an increase in sinuosity from 2006 to 2019, with the most significant increase following the large flood of 2011. Sinuosity for the lower reach also increased in 2015 (Figure 14). Sinuosity increased from 2006-2019 for the upper reach but did not increase following the large flood of 2011 (Figure 14; Figure 15). Sinuosity for the middle reach increased from 2006 to 2013, then decreased from 2013 to 2019 (Figure 14). All three LW reaches increased before the large flood. The control reach showed little to no change in sinuosity from 2006 to 2019 (Table 1).

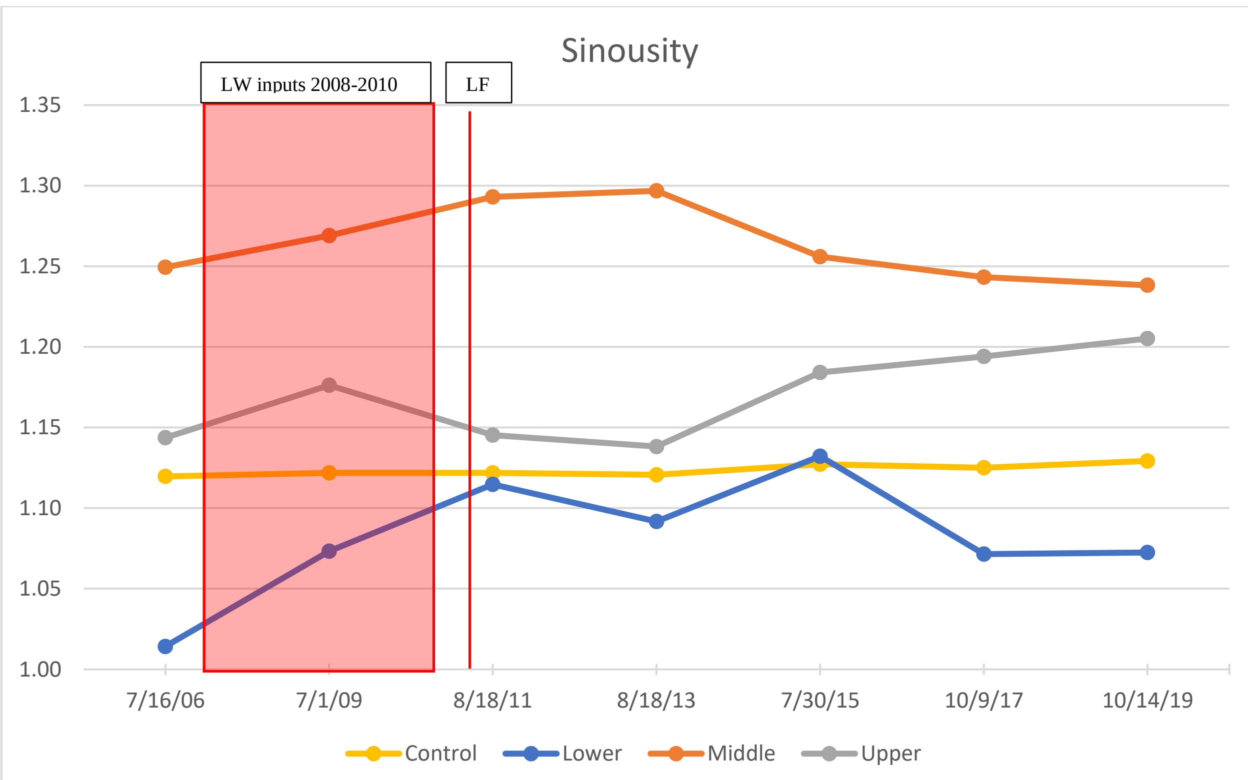


Figure 14: The sinuosity values calculated for all four study reaches from the years 2006 to 2019. The red shaded box indicates the large wood addition timeframe. The red line indicates the large flood (LF).

Table 1: The values determined for the sinuosity and the multi-threaded channel index

| **Threaded Channel Index** | | | | | **Sinuosity** | | | |
|---|---|---|---|---|---|---|---|---|
| | Control | Lower | Middle | Upper | Lower | Middle | Upper | Control |
| **7/16/06** | 1.12 | 1.10 | 1.25 | 1.19 | 1.01 | 1.25 | 1.14 | 1.12 |
| **7/1/09** | 1.12 | 1.15 | 1.32 | 1.24 | 1.07 | 1.27 | 1.18 | 1.12 |
| **8/18/11 *year of large flood** | 1.12 | 1.86 | 2.14 | 1.91 | 1.11 | 1.29 | 1.15 | 1.12 |
| **8/18/13** | 1.12 | 1.90 | 2.07 | 1.91 | 1.09 | 1.30 | 1.14 | 1.12 |
| **7/30/15** | 1.13 | 1.95 | 1.85 | 2.14 | 1.13 | 1.26 | 1.18 | 1.13 |
| **10/9/17** | 1.13 | 1.91 | 1.84 | 2.07 | 1.07 | 1.24 | 1.19 | 1.13 |
| **10/14/19** | 1.13 | 1.96 | 1.73 | 2.11 | 1.07 | 1.24 | 1.21 | 1.13 |

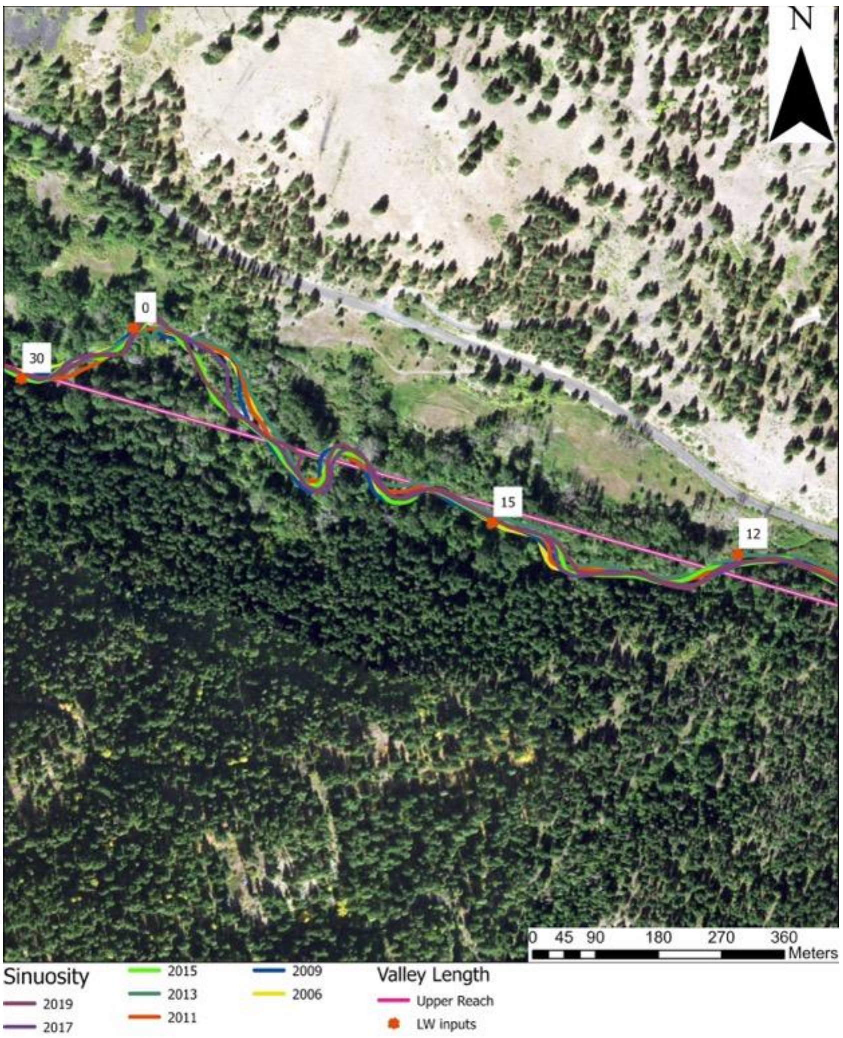


*Figure 15: An example of the sinuosity measurements at the upper reach. The numbers next to the LW inputs are the number of LW pieces. The straight pink line represents the valley length.*

## Multi-Threaded Channel Index

The multi-threaded channel index increased significantly for all three reaches following the large flood of 2011. The lower reach increased and stayed relatively stable, while the middle reach increased after the large flood, then decreased over time (Figure 16; Figure 17). The upper reach increased after the large flood and continued to increase over time (Figure 16). The control reach saw no new multi-threaded channels from 2006-2019, and therefore did not change over time (Table 1).

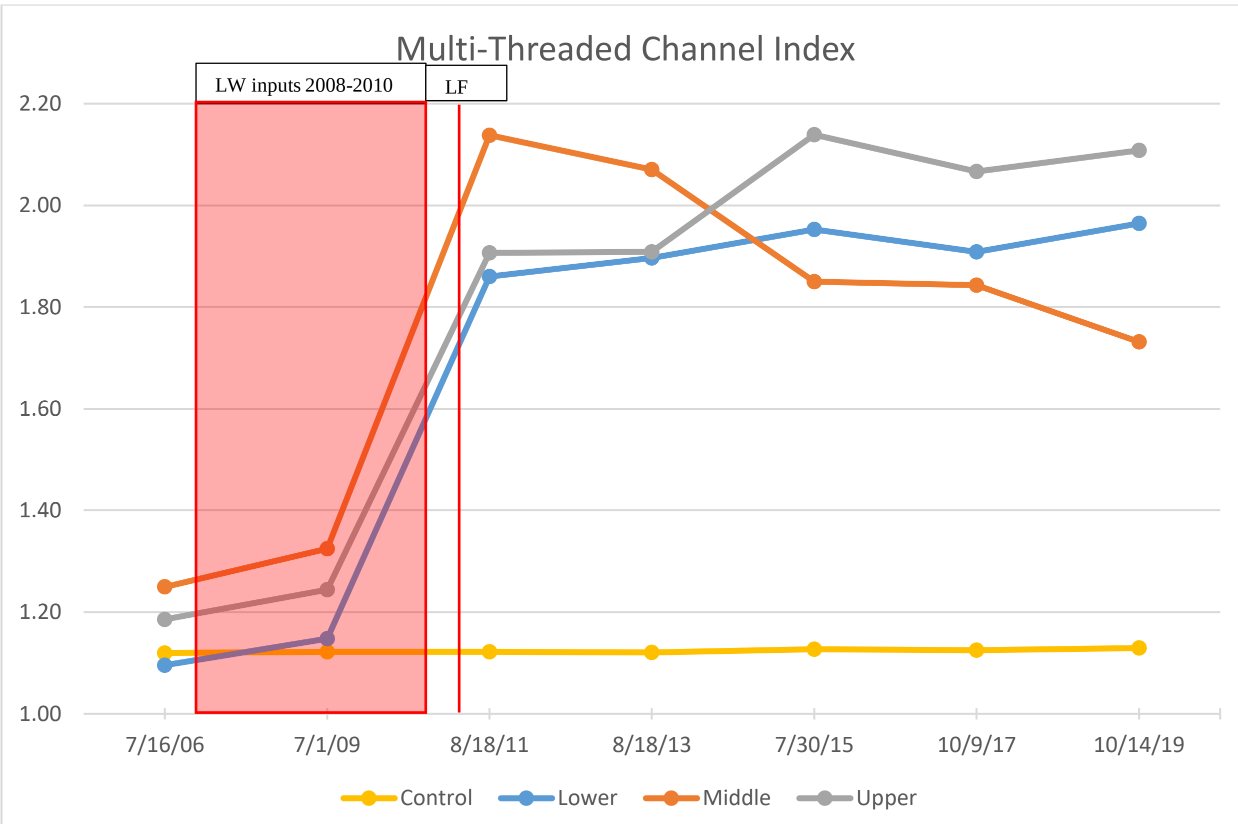


Figure 16: The multi-threaded channel index values calculated for all four study reaches from the years 2006 to 2019. The MCI increased at the three reaches with LW after the large flood of 2011, but not in the control reach. The red shaded box indicates the large wood addition timeframe. The red line indicates the large flood.


*Figure 17: The MTCI for the middle reach. The numbers next to the LW inputs indicate the number of LW pieces.*

The drone imagery for the three LW reaches showed side channels in proximity to LW jams. In the lower reach, 6 side channels were identified and four LW jams were within 10 m downstream of these jams. In this reach, 66% of the side channels were formed within 10 m of the LW jams. In the middle reach, six side channels were identified and five side channels were formed within 10 m of the LW jams. In this reach, 83% of the side channels were formed within 10 m of the LW jams. In the upper reach, nine side channels were identified and six side channels were formed within 10 m of the LW. In this reach, 66% were formed within 10 m of the LW jams.

## Normalized Difference Vegetation Index

All three study reaches showed similar NDVI greenness values from 2006 to 2011, with a general increasing trend. The control reach produced values that were consistently 0.04 lower than the study reaches from 2006 to 2011 (Figure 18). All four reaches increased significantly in 2012 in greenness one year after the large flood in 2011 (Figure 18). The years following the large flood, from 2013 to 2019 showed a slight increase in greenness for all four reaches compared to before the flood (Figure 18). The four reaches followed the same general trend, with some years drier than others, however the three study reaches saw more dynamic change and increased in difference compared to the control reach (Table A1).

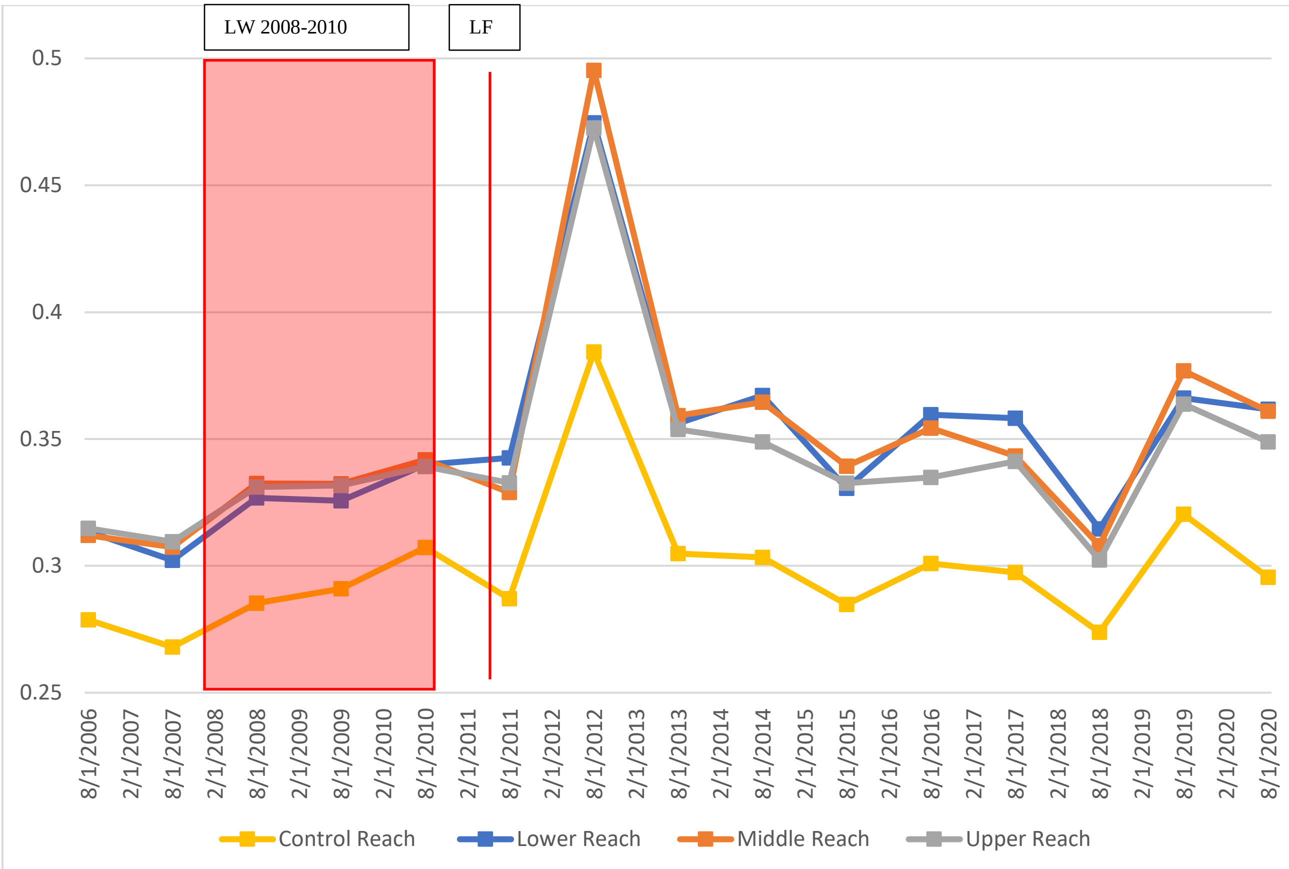


Figure 18: The NDVI values calculated for the study reaches and their respective floodplains. All four study reaches saw increases in floodplain greenness, however the LW reaches experienced larger increases than the control reach (Table A1). The red shaded box indicates the large wood addition timeframe. The red line indicates the large flood (LF).

## Piezometer Analysis

The lower reach contained a total of 11 piezometer measurements where values ranged from -0.9 cm to 4 cm. Downstream of the beaver dam (Figure 6) upwelling of 1cm occurred in the riffle, followed by slight upwelling on 0.7 cm in the pool created by the LW (Figure 19). Upwelling occurred most notably in the deep pools within the large wood structures with values of 3 cm and 4 cm (Figure 19). Downwelling was present in the riffles downstream of the log jams.

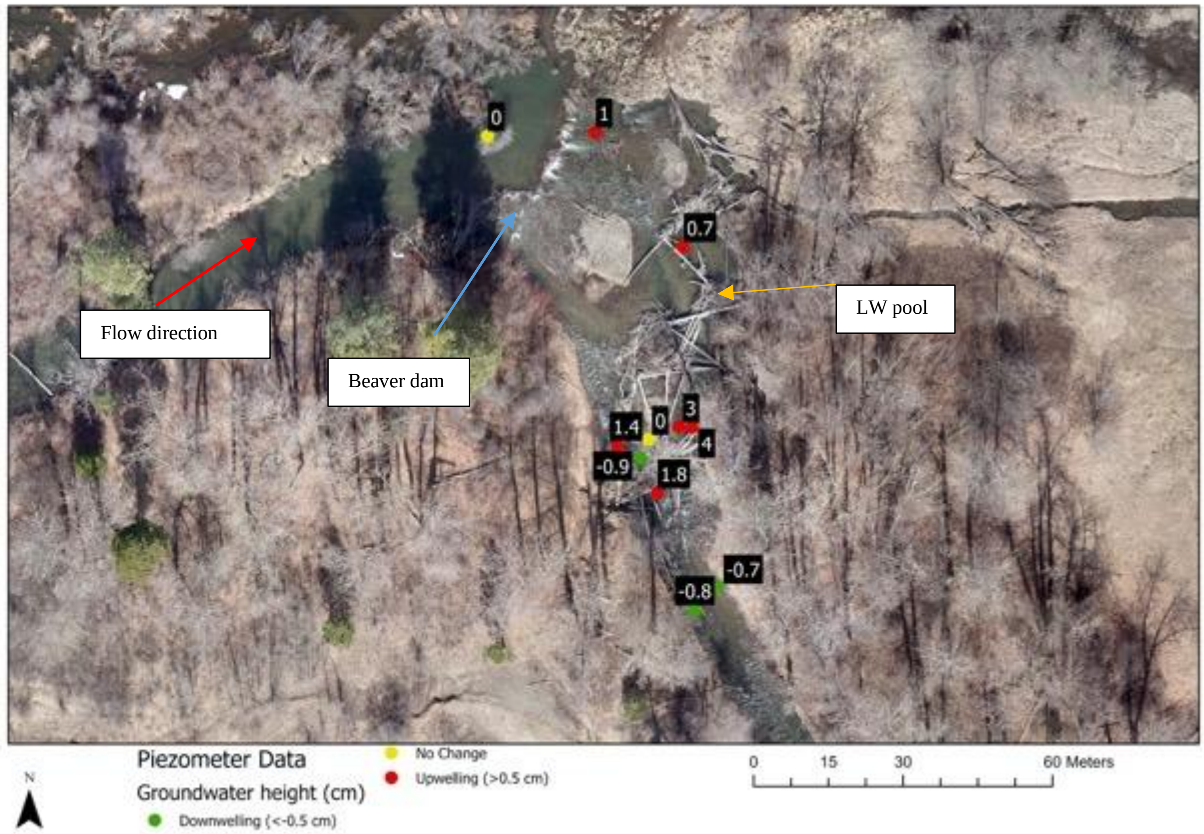


Figure 19: The piezometer upwelling (positive numbers) and downwelling (negative numbers) data for the lower LW reach (Figure 6). Upwelling occurred in LW pool and below the beaver dam, annotated in red, while downwelling occurred in the riffles. The red arrow indicates flow direction. The blue arrow indicates a beaver dam. The yellow arrow indicates a LW pool.

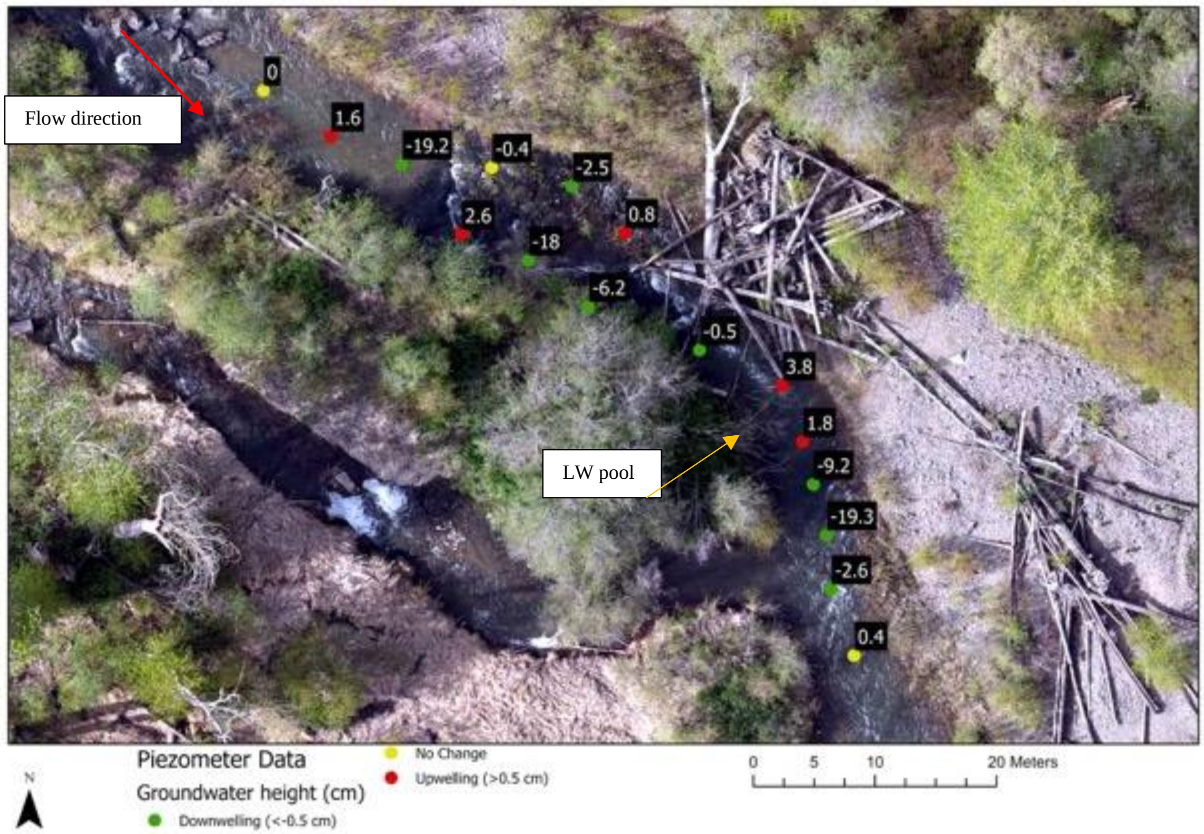


Figure 20: The piezometer upwelling (positive numbers) and downwelling (negative numbers) for the middle LW reach (Figure 6). Upwelling occurred in LW, annotated in red, while downwelling occurred in the riffles. The red arrow indicates flow direction. The yellow arrow indicates a LW pool.

A total of 16 piezometer measurements were taken at the middle reach and measurements varied from several cm to almost 20 cm of downwelling. Upwelling occurred within approximately 10 m downstream of the log jam and 5 m upstream of the log jam on the left bank (Figure 20). Some upwelling occurred at the furthest upstream end of the reach, downstream of the boulder cluster. Downwelling occurred in the riffle downstream of the large wood jam and in the riffle upstream of the log jam. Bed material consisted of cobbles, gravels, silty sands, and some organics. Measurements recorded within +/- 0.5 cm or less were described as no change. It is possible that high negative downwelling values clogged.

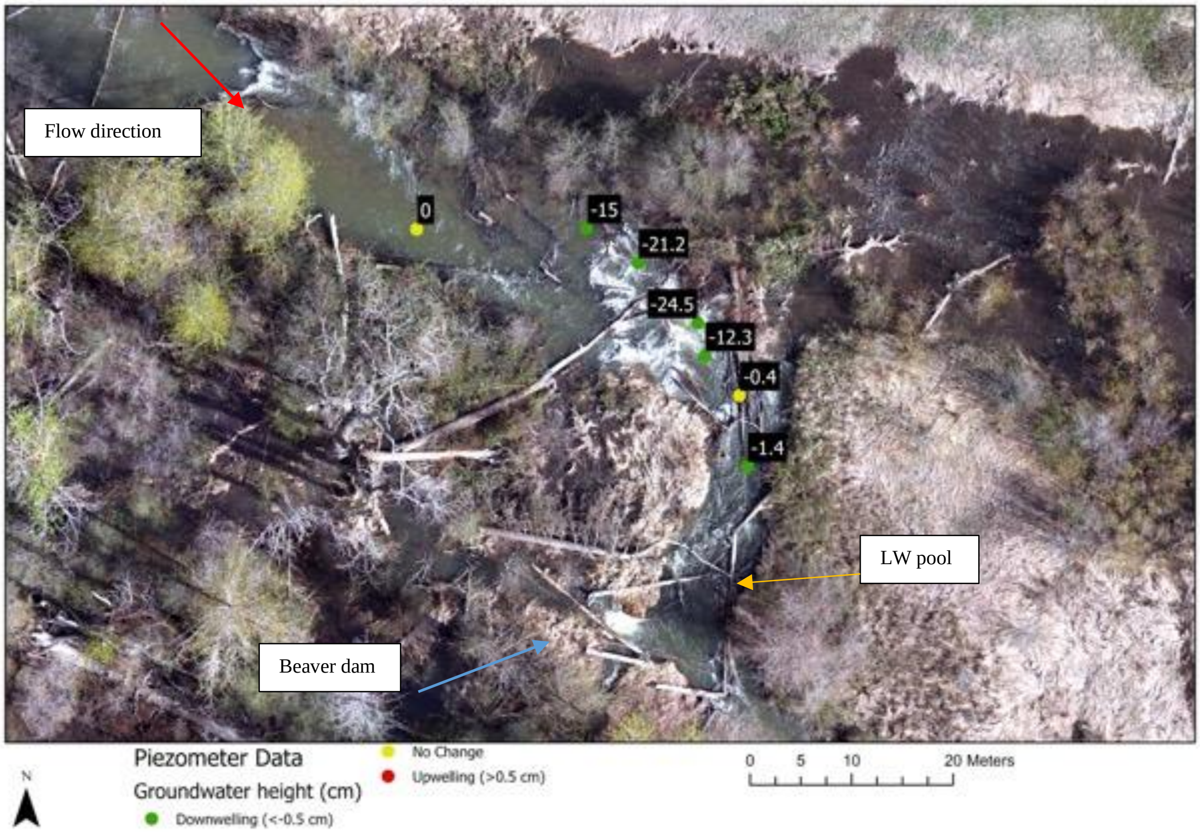


Figure 21: The piezometer upwelling and downwelling data for the upper LW reach (Figure 6). Only downwelling occurred at this reach, measurements might have been influenced by a confining clay layer.

A total of seven piezometer measurements were taken at the upper reach where all measurements recorded downwelling or no change. The furthest downstream measurement in the riffle within the large wood contained mostly cobble substrate and yielded 1.4 cm of downwelling (Figure 21). The other measurements taken within this reach saw significant downwelling, ranging from 12.3 to 24.5 cm (Figure 21). These sites contained a blue clay layer estimated to be 50 cm or more, the piezometer likely never broke through this layer. Measurements recorded within +/- 0.5 cm or less were described as no change. It is possible that high negative downwelling values clogged.

## Salinity and Temperature Analysis

Cross-sectional measurements were conducted at the Lower Reach for temperature and salinity, however the tight spacing of the log jams did not allow for precise cross-sectional measurements across the stream. The data collected was too widely spaced along the cross-sections to allow for proper interpolation.

The salinity of the middle reach was higher at the LW jam and just downstream of the LW. The left bank recorded higher salinity than the right bank downstream of the LW jam. Immediately upstream of the LW jam salinity decreased for approximately 10 m, then increased upstream for approximately 10 m. The temperature of values upstream of the LW were all within relatively uniform and around 3$^{o}$C warmer. The cross-sections downstream of the LW jam show variability in salinity values than upstream of the LW jam.


Figure 22: The salinity values μS/cm for the Middle Reach LW reach. The salinity values were higher on the immediately downstream of the LW and on the left bank. The blue arrow indicates the location of the LW jam.

The salinity of the middle reach was lower upstream of the LW jam and higher just downstream of the LW (Figure 22). There was little variability in salinity throughout the rest of the reach suggesting that the water is well mixed and there is not significant patchiness due to strong upwelling zones.

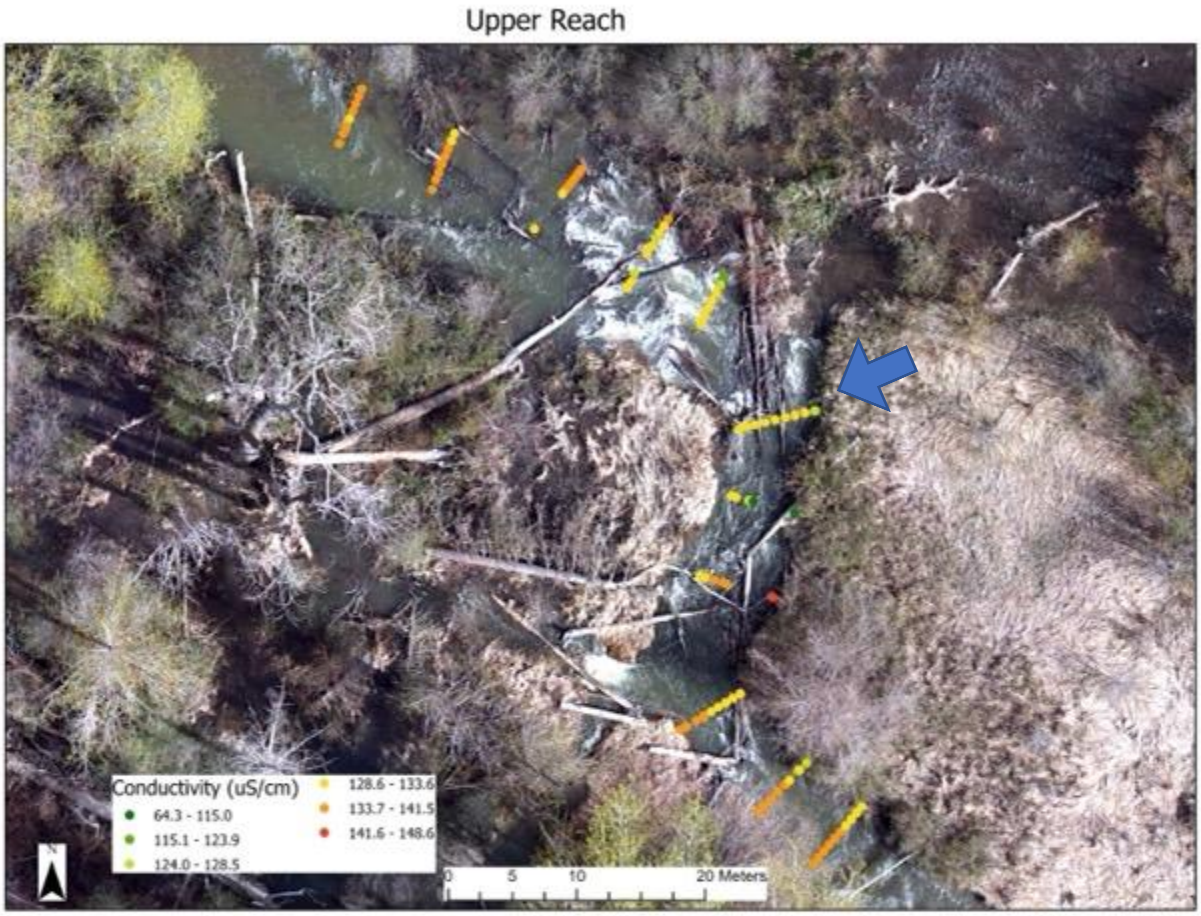


Figure 23: The salinity values µS/cm for the upper LW reach. The salinity values remained relatively consistent, except for the extremely high and low values found on the left bank. The blue arrow indicates the location of the LW jam.

## Beaver Dam Analysis

In the lower reach, five large beaver dams ranging from approximately 40-80 m in length were mapped, with 11 additional small beaver dams mapped where connectivity between them could not be determined. The extent of the newly created wetland was also determined, with inputs identified as two side channels from the west and two outputs into Taneum creek identified in the east (Figure 23).

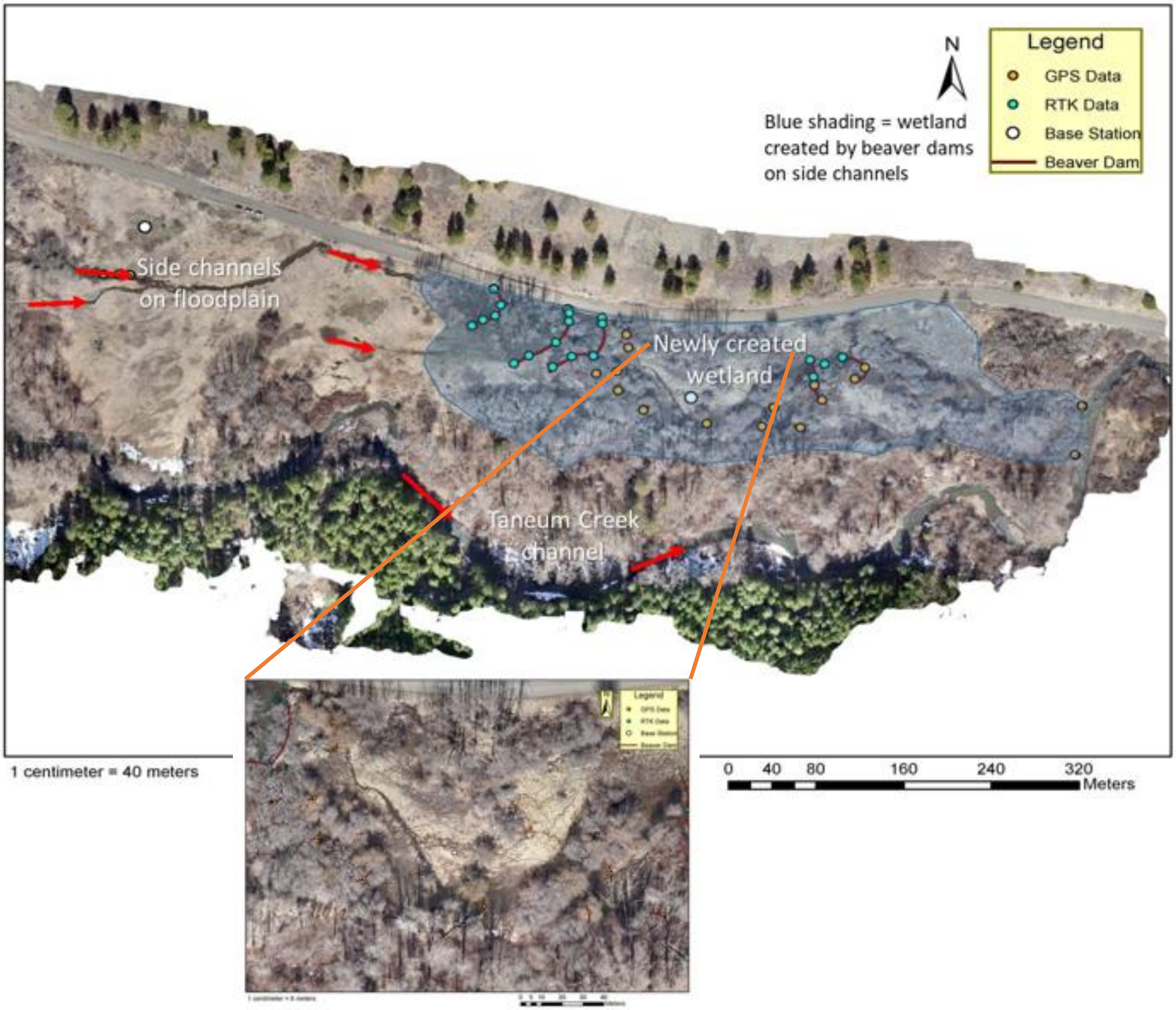


Figure 24: The beaver dams' lengths and locations were mapped at the lower reach. Beaver dams were only found in the wetland complex shaded in blue. Inset photo shows the wetland complex and beaver dam at a smaller scale.

# CHAPTER V

## DISCUSSION

Large wood plays a critical role in modifying channel morphology at a fine resolution, however there is debate on its impacts at a larger scale across floodplains. Taneum Creek experienced significant channel changes following the large flood of 2011 in the reaches with large wood additions. The change in NDVI affected the entire study site to some extent but remained consistently lower in the control reach than in the LW reaches. The salinity and piezometer data showed mixed results but suggest an interaction downstream of LW jams.

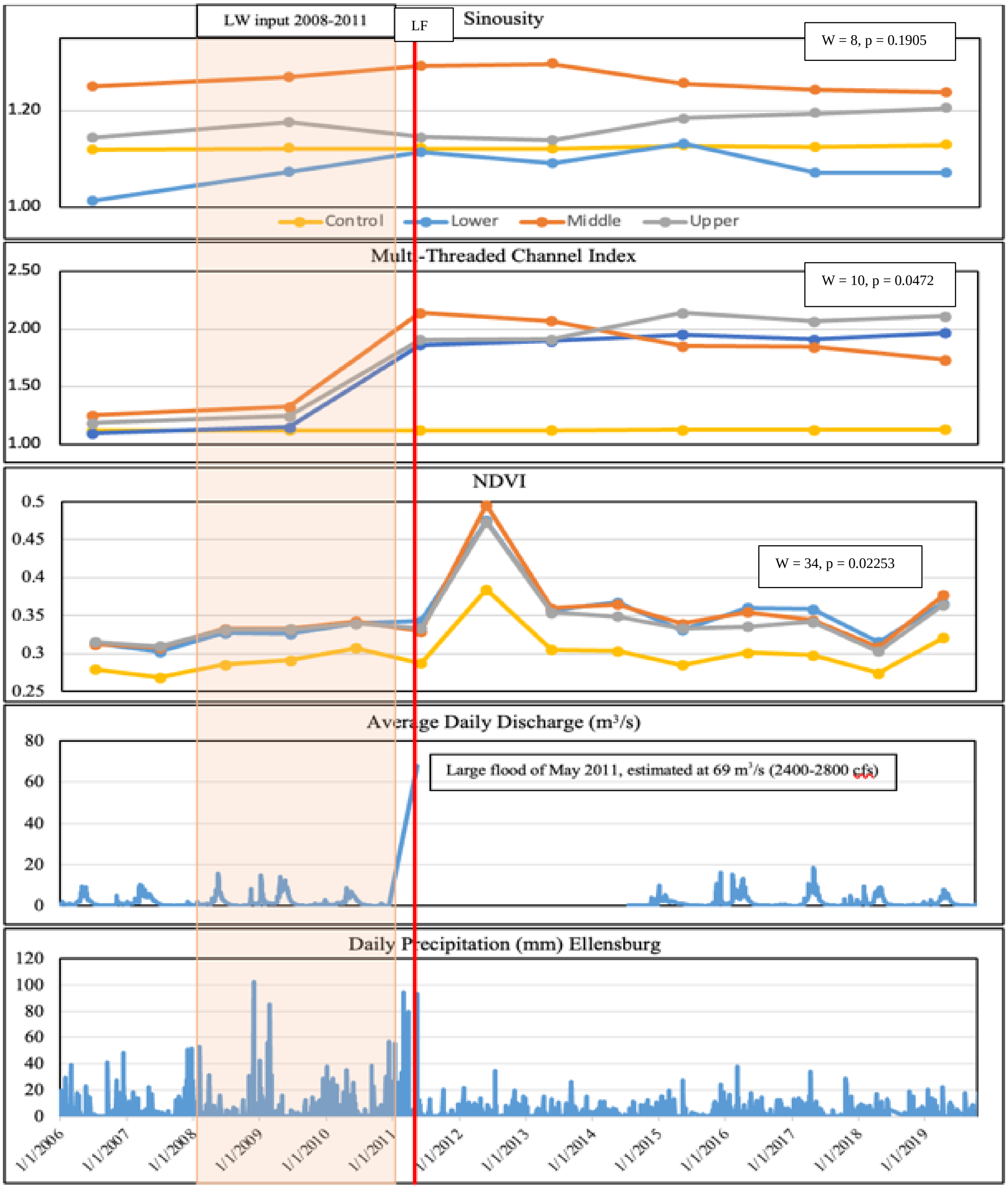


Figure 25: The sinuosity, multi-threaded channel index, and NDVI values compared to the daily precipitation and Taneum Creek average stream discharge. The orange-shaded box represents the LW input, and the red line and indicates the date of the large flood (LF) of 2011. Mann-Whitney U test was conducted for significant great than difference at LW reaches before and after the large flood.

The increase in the channel sinuosity of the three LW reaches following the 2011 flood was slight, but noticeable, however not statistically significant (Figure 26). The increase in the upper reach lagged behind the other LW reaches, suggesting a varied connection between LW and increases in channel sinuosity. The introduction of beaver activity in the upper reach might be one explanation for the later increases in sinuosity. One common characteristic of the lower and middle reaches was the gradual decrease in sinuosity in the years following the initial peak after the 2011 flood. This suggests that the channel might have gradually re-incised, or that the river could have established more direct paths through the log jams. The control reach did not experience any noticeable sinuosity channel changes after of the large flood.

The LW study reaches saw significant increases in their respective multi-threaded channel indices (MTCI) following the large flood of 2011 (W= 10, alternative = “greater, p = 0.04762;), while the control reach did not differ from its sinuosity index (R Core Team, 2020). The LW reaches did not see a significant difference in sinuosity when compared to before and after the large flood (W = 8, alternative = “greater, p = 0.1905; R Core Team, 2020). The increases in the LW reaches suggest that the LW played a role in the formation of new side channels. The large flood did not alter the channel in any noticeable way in the control reach. The multi-threaded channel indices for all three LW reaches have remained at new values that were higher than before the 2011 flood. In the lower and upper reaches, 66% of the side channels were formed within 10 meters downstream of a LW jam after the large flood. In the middle reach 83% of the side channels were formed within 10 meters downstream of a LW jam. This suggests that LW was responsible for greater than 50% of the side channels avulsions in all three reaches following the large flood. The proximity of the side channels to LW jams indicates that LW played an important role in side channel creation during the large flood of 2011.

There are slight differences among the reaches, for example in the upper and lower reaches, the MTCI increased following the large flood, and settled in a more stable but higher configuration, whereas in the middle reach the MTCI peaked and then settled at a slightly lower value as channel configuration stabilized or as some channels were abandoned. One possible explanation is the presence of beavers in the lower and upper reaches (Figure 25), which stabilized the formation and longevity of these side channels. Another explanation is a decrease in stream slope, which would impact beaver colonization. In the middle reach, side channel creation did produce channels small enough for beaver colonization in the middle of the reach. The control reach has no side channels and the main channel of Taneum Creek is generally too energetic for dam construction. So, if there are no side channels there are likely no beaver dams. The incision of the control reach likely yields channel geometry that does not allow beaver colonization. The higher valley walls and terraces of the control reach might also be a contributing factor in the control reach, thus limiting beaver activity. The geometry of the stream channels in the upper, middle, and lower reaches is less incised, resulting in greater floodplain connectivity, side channel creation, and increased floodplain inundation. These factors might not have been present before the large flood and the LW additions, suggesting the increase in beaver habitat because of these variables.

The NDVI values for the three study reaches and control reaches increased in the floodplains the year following the large flood (2012), likely a result of flood disturbances in the system. The flood of 2011 likely exposed the soil and deposited nutrients during the summer of 2011, likely causing a decrease in NDVI values. Then in 2012, the new plant growth forbs signal increased greenness in the imagery. The new side channels created by the flood would bring more water out onto the floodplain after 2011, and 2012 was a wet summer, which could have contributed to the high greenness everywhere (Figure 27). Average NDVI values for all LW. reaches were significantly greater (W = 34, alternative = “greater”, p = 0.02253) than the values before the large flood. (R Core Team, 2020; Figure 28). The control reach was not significantly greater in NDVI values when compared to before and after the large flood event (W = 27, alternative = “greater”, p = 0.1772). The control reach decreased closer to its formed greenness values, but the beaver ponds and side channels in LW reaches might play a greater role in maintaining floodplain moisture and higher greenness during drier years.

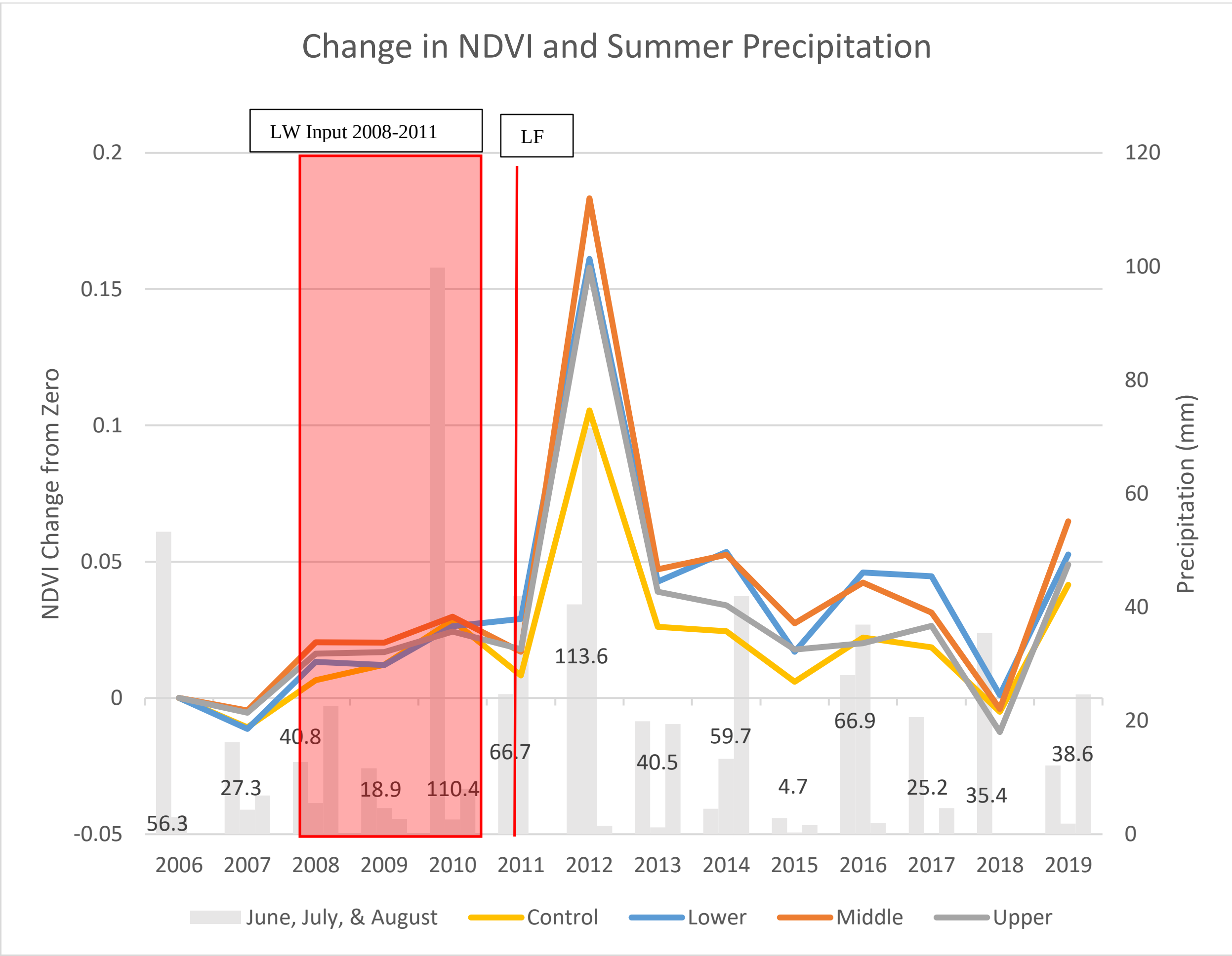


Figure 26: The calculated NDVI values (line graph) represented as the change from the measurement on the starting date. The precipitation data (bar graph) from Ellensburg, WA during the summer months. The values represent the sum of the three months for each year. The shaded box represents the LW addition timeframe, and the vertical red line represents the large flood (LF) of 2011.

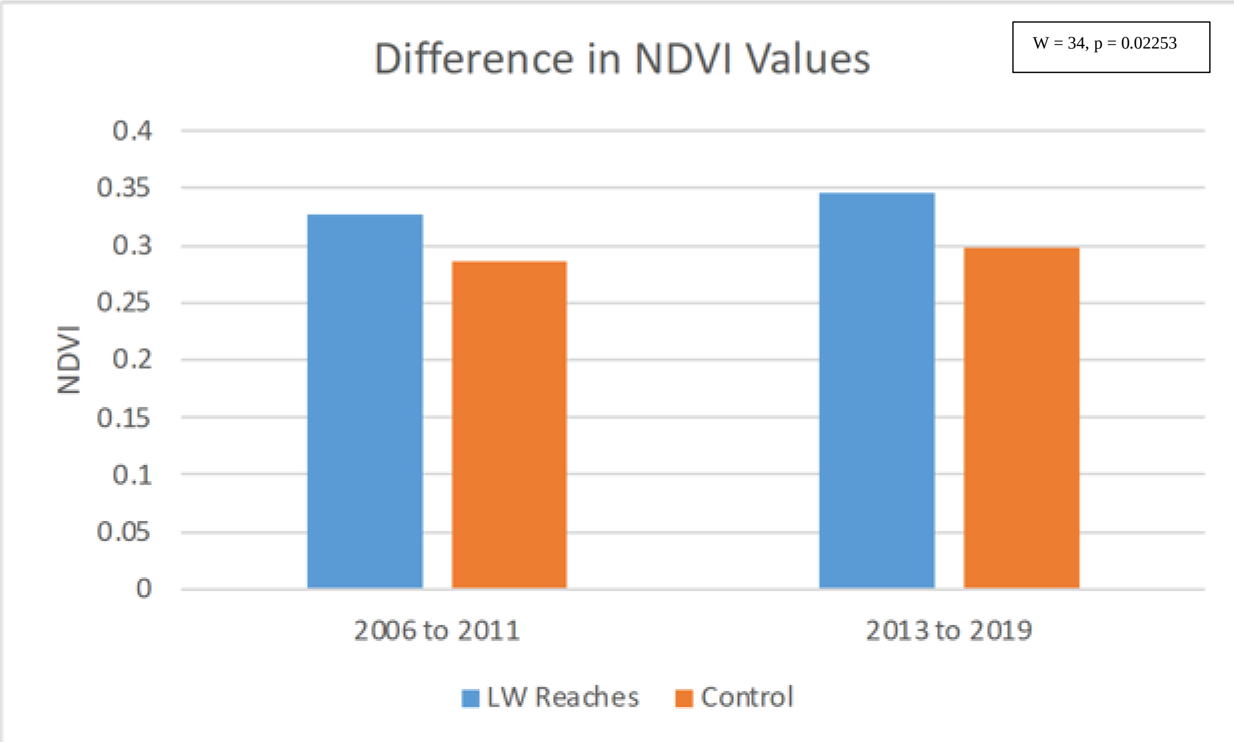


Figure 27: The average NDVI values for all LW reaches compared to the control reach. The year of 2012 was excluded. The LW study reach NDVI values after the large flood were significantly greater when compared to the values before the large flood.

While the control reach also increased in greenness on the floodplain, the increases in the LW reaches were nearly double the increases found in the control reach. This is likely a result of the channel avulsions created in the LW reaches, where the control reach did not see any new channel formations. The wet summer of 2010 does not coincide with a large increase in greenness as seen in 2012 (Figure 29). This might be a result of the timing of the moisture in June 2010 and July 2012 because July rain might have a greater effect on the August imagery. This might suggest that the combination of side channel creation in the floodplains of the LW and the high precipitation of that summer created a high greenness value for all the LW reaches. The NDVI values for the control reach and the three LW reaches were fairly similar before the 2011 flood and again after 2018. However, for the six years following the flood, from 2012-

2017, the NDVI values of the three LW reaches remained consistently higher than for the control reach. These results suggest that the transfer of water onto the floodplain through the side channels might have increased retention of summer moisture in the floodplain for several years after they were created. Why this difference between the LW reaches and the control reach diminished after 2018 remains open to question.

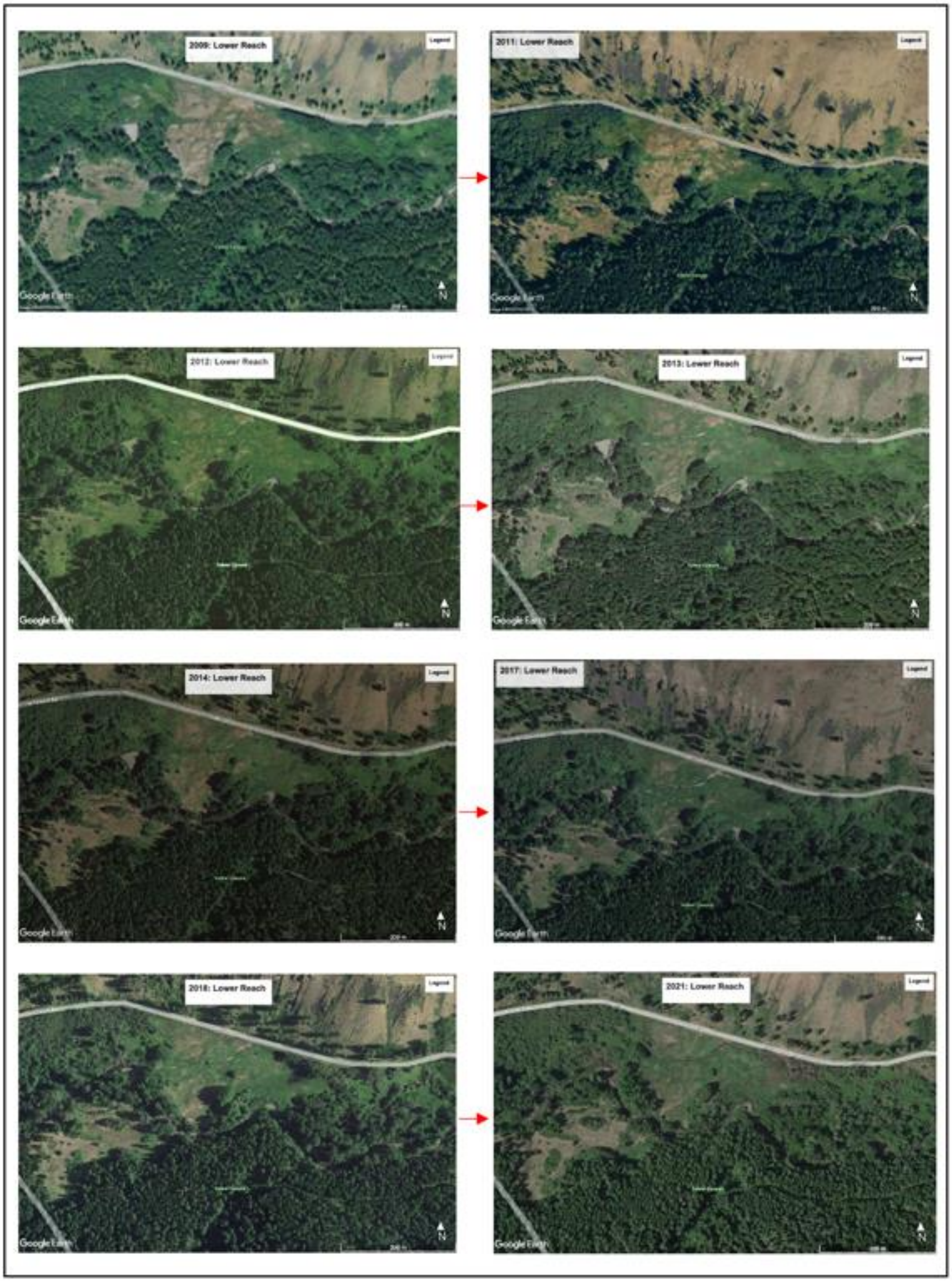


Figure 28: The floodplain of the lower LW reach of Taneum Creek over the course of 12 years. The floodplain during the year of 2012 appears to be much greener than other years, indicating that the NDVI values for 2012 do accurately represent the spike in greenness.

## Piezometer and Salinity Study

The piezometers temporarily placed in the LW reaches illustrated variable upwelling and downwelling conditions near the LW additions (Figure 23 and 24). The lower reach did not see correlating piezometer data, while both the middle and upper reaches showed mixed indications of downwelling and upwelling. The data recorded at the upper reach is likely significantly impacted by the presence of a blue clay layer which might confine the groundwater interaction and produce erroneously large downwelling values if the piezometer extended below the clay layer (Figure 20). However, in the middle reach, downwelling was observed in the riffle downstream the pool and the LW jam, likely created by the large wood pool-riffle sequence (Thompson and Fixler, 2017). The pool immediately downstream of the LW showed some upwelling, which was also observed in the LW pools in the lower reach. Downwelling less than 1cm also occurred in the riffle sequences in the lower reach, but the differences of less than 1 cm are below the confidence level of the measurements. The downwelling might be a product of the increased slopes typical of riffle systems. Left bank upwelling values found in the middle reach might be a result of valley slope groundwater intrusion. The cross-sectional data for lower reach was not precise to the locations of the cross-section tape because the LW jam made data collection every 0.5m impossible, resulting in data that was unable to be interpolated.

The temperature data for all three LW study reaches was deemed inconclusive, with no discernable pattern present at the LW sites. However, the salinity data recorded in the middle reach indicates upwelling within 5m downstream of the LW jam, which is consistent with the upwelling found in the piezometer data in that area (Figure 30).

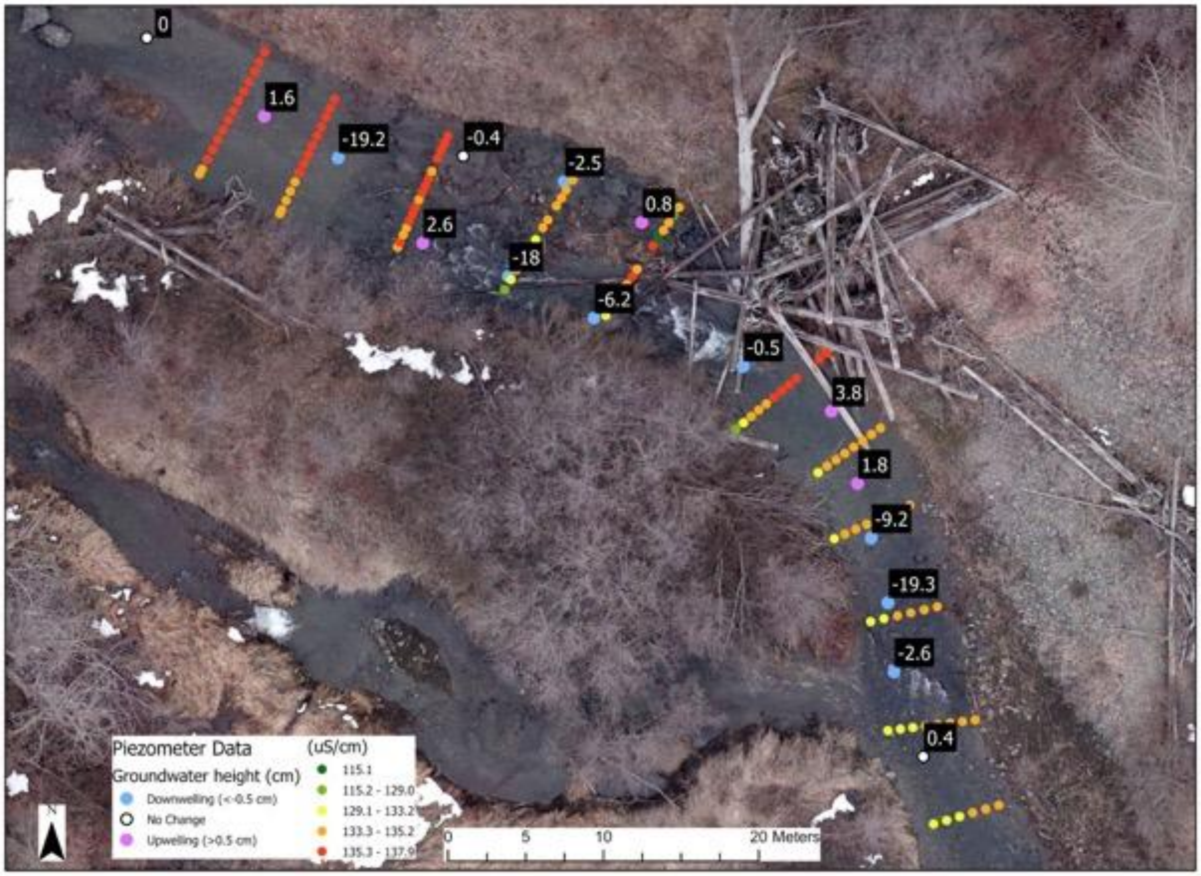


Figure 29: The combination figure of the salinity data and piezometer data for the middle reach.


Figure 30: The combination figure of the salinity data and piezometer data for the upper reach. The yellow arrow indicates the LW pool, and the red arrow indicates the LW jam.

In the upper reach, the salinity values followed are fairly uniform except for the two lone deviations found downstream of the LW jam and at the LW pool. High pattern immediately downstream of the pool is similar to the pattern found in the middle reach. (Figure 31). The pattern of low to high salinity immediately which could be an error in the data because of the extremely low conductivity value of 64.3 uS/cm (Figure 31). The general pattern of salinity downstream of the LW jam is consistent with the data found in the middle reach downstream of the LW jam, if the low salinity value is not erroneous. The piezometer data in this reach is most likely skewed starting upstream from the -12.3 cm of downwelling found in the upper portion of the reach (Figure 31).

In general, the high and low salinity values did not correspond with the upwelling and downwelling seen in the piezometer measurements. The only salinity values that corresponded with the upwelling and downwelling were immediately downstream of the LW jams at both sites in the pool-riffle sequences. This suggests that downwelling and upwelling follow a pattern of upwelling at the downstream end of pools, following downwelling in the riffles. The LW pool-riffle coupling indicates localized groundwater movement that might be confined to less than one meter. Methodology should be revised to improve piezometer design. The cobble bed of Taneum Creek resulted in unorganized placement of the piezometer, creating some inconclusive data. The salinity and temperature probe suffered from some data collection issues, however, the cross-section transects established showed potential in identifying areas of upwelling. Ideally, measurements should be taken every 0.25 m instead of every 0.5m to improve accuracy. The capacity of the conductivity and temperature reach wide survey was limited by the number of errors related to moving around LW jams. Subsequently this method is not suggested for future studies on small shallow streams with numerous obstacles.

The implications of the interactions of the LW and the groundwater upwelling and downwelling within the channel from the piezometer and salinity/temperature measurements are inconclusive. But it is possible that LW forced pool-riffle coupling could create some more complex groundwater interactions.

# CHAPTER VI

# CONCLUSION

The importance of large wood (LW) in creating channel complexity is widely recognized; however, few LW projects have been in place long enough to track meaningful channel changes on a decadal timescale. This project addressed the long-term effects of LW restoration on channel changes, floodplain connectivity, and groundwater-surface water interactions. The results indicate that LW in combination with a large flood creates channel complexity by increasing sinuosity, multi-threaded channel index (MTCI), beaver activity, and floodplain connectivity. The LW might not have had as great an effect if there had not been a large flood, especially because some of the LW was originally placed above the elevation of the channel banks. Large wood floodplain restoration at Indian Creek, located in central WA did not have a large flood event and there have been no significant channel changes in six years (Bartlett, 2022)

The interaction between LW and in-stream groundwater was not fully realized; however, there is an indication that forced LW pool-riffle coupling downstream of LW jams could have some more complex interactions worthy of future study. The most important result highlighted by this research was the drastic increases in MTCI following the large flood of 2011 in the reaches were LW was restored. Additionally, the spike in NDVI data demonstrates the change in channel habitat connectivity and vegetation potential. The increase in floodplain inundation resulted in increases in floodplain greenness and new vegetative growth following the large flood.

These channel avulsions and the occupation of side channels allowed for increased summer floodplain greenness, channel complexity, and beaver colonization. It appears that LW can be a factor in the creation of side channel avulsions.

Future research should focus on the interactions of LW and groundwater in the floodplain and within the stream channel. The piezometer and salinity/temperature measurements showed promise, but methodology could be revised to improve piezometer design.

The potential for LW restoration projects to create changes in channel geomorphology, habitat, and groundwater is clearly represented by the results of this project. The benefits of LW and allowing natural channel processes to take place highlight the potential of LW restoration to improve various water management endeavors, ecological functions, and channel complexity.

## REFERENCES


Abbe, T. B. and Brooks, A., 2011, Geomorphic, engineering, and ecological considerations when using wood in river restoration. In Stream Restoration in Dynamic Fluvial Systems: Scientific Approaches, Analyses, and Tools American Geophysical Union Washington, DC, vol. 194, p. 419-451.

Abbe, T.B. and Montgomery, D.R., 1996. Large woody debris jams, channel hydraulics and habitat formation in large rivers. Regulated Rivers: research & management, no 2-3, p. 201-221.

Abbe, T.B. and Montgomery, D.R., 2003, Patterns and processes of wood debris accumulation in the Queets River basin, Washington. Geomorphology, no. 1-3, p. 81-107.

Bartlett, S., 2022, Assessing the Effects of Instream Large Wood on Floodplain Aquifer Recharge and Storage at Indian Creek, Kittitas County, Washington, USA, *All Master's Theses*. 1735. https://digitalcommons.cwu.edu/etd/1735

Beechie, T., Imaki, H., Greene, J., Wade, A., Wu, H., Pess, G., Roni, P., Kimball, J., Stanford, J., Kiffney, P. and Mantua, N., 2013, Restoring salmon habitat for a changing climate. River research and applications, no. 8, p. 939-960.

Beechie, T.J. and Sibley, T.H., 1997, Relationships between channel characteristics, woody debris, and fish habitat in northwestern Washington streams. Trans. Am. Fish. Soc., v. 126 p. 217-229

Beschta, R.L., 1979, Debris removal and its effect on sedimentation in an Oregon Coast Range stream. Northwest Sci., v. 53, p. 71-77.

Boylan, N. C., 2019, Assessing the Link Between Large Wood Restoration and Groundwater Recharge and Storage: An Investigation of Indian Creek in Washington

State.https://ir.library.oregonstate.edu/concern/graduate_thesis_or_dissertations/5425kh99

Chin, A., Daniels, M. D., Urban, M. A., Piégay, H., Gregory, K. J., Bigler, W., ... and Wohl, E., 2008, Perceptions of wood in rivers and challenges for stream restoration in the United States. Environmental management, no. 6, p. 893-903.

Collins, B. D., Montgomery, D. R., Fetherston, K. L., and Abbe, T. B., 2012, The floodplain large-wood cycle hypothesis: A mechanism for the physical and biotic structuring of temperate forested alluvial valleys in the North Pacific coastal ecoregion. Geomorphology, v. 139, p. 460-470.

Collins, B.D. and Montgomery, D.R., 2002, Forest development, wood jams, and restoration of floodplain rivers in the Puget Lowland, Washington. Restoration Ecology, no. 2, p. 237 247.

Comiti, F., Lucía, A. and Rickenmann, D., 2016, Large wood recruitment and transport during large floods: a review. Geomorphology, v. 269, p. 23-39.

Dolloff, C.A. and Warren, M.L., 2003., Fish relationships with large wood in small streams. In American Fisheries Society Symposium 37: 179-193, 2003.

Ely, D.M., Bachmann, M.P., and Vaccaro, J.J., 2011, Numerical simulation of groundwater flow for the Yakima River basin aquifer system, Washington: U.S. Geological Survey Scientific Investigations Report 2011-5155, 90 p.

Fetherston, K. L., Naiman, R. J., and Bilby, R. E., 1995, Large woody debris, physical process, and riparian forest development in montane river networks of the Pacific Northwest. Geomorphology, v. 13, p. 133-144

Friend, P.F., and Sinha, R., 1993, Braiding and meandering parameters: Geological Society, London, Special Publications, v. 75, p. 105–111.

Gergel, D. R., Nijssen, B., Abatzoglou, J. T., Lettenmaier, D. P., and Stumbaugh, M. R., 2017, Effects of climate change on snowpack and fire potential in the western USA. Climatic Change, no. 2, p. 287-299.

Gendaszek, A.S., Ely, D.M., Hinkle, S.R., Kahle, S.C., and Welch, W.B., 2014, Hydrogeologic framework and groundwater/surface-water interactions of the upper Yakima River Basin, Kittitas County, central Washington: U.S. Geological Survey Scientific Investigations Report 2014 5119, 66 p., http://dx.doi.org/10.3133/sir20145119.

Gonzalez, R., Dunham, J., Lightcap, S. and McEnroe, J., 2017, Large wood and instream habitat for juvenile Coho salmon and larval lampreys in a Pacific Northwest stream. North American Journal of Fisheries Management, no. 4, p. 683-699.

Grabowski, R.C., Gurnell, A.M., Burgess-Gamble, L., England, J., Holland, D., Klaar, M.J., Morrissey, I., Uttley, C. and Wharton, G., 2019, The current state of the use of large wood in river restoration and management. Water and Environment Journal, no 3, p. 366 377.

Gurnell, A.M., Piégay, H., Swanson, F.J. and Gregory, S.V., 2002, Large wood and fluvial processes. Freshwater Biology, no. 4, p.601-619.

Hong, L.B., and Davies, T.R.H., 1979, A study of stream braiding: Geological Society of America Bulletin, v. 90, p. 1839–1859.

Hümann, M., Schüler, G., Müller, C., Schneider, R., Johst, M., & Caspari, T., 2011, Identification of runoff processes–The impact of different forest types and soil properties on runoff formation and floods. Journal of Hydrology, no. 3-4, p. 637-649.

Jencso, K. G., McGlynn, B. L., Gooseff, M. N., Wondzell, S. M., Bencala, K. E., and Marshall, L.A., 2009, Hydrologic connectivity between landscapes and streams: Transferring reach and plot-scale understanding to the catchment scale. Water Resources Research, no. 4, https://doi.org/10.1029/2008WR007225

Johnston, C. A., 2014, Beaver pond effects on carbon storage in soils. Geoderma, vol. 213, p. 371-378.

Jones, K.K., Anlauf-Dunn, K., Jacobsen, P.S., Strickland, M., Tennant, L. and Tippery, S.E., 2014, Effectiveness of instream wood treatments to restore stream complexity and winter rearing habitat for juvenile coho salmon. Transactions of the American Fisheries Society, no. 2, p. 334-345.

Jones and Stokes Associates, 1991, Watershed characteristics and conditions inventory; Taneum Creek and Tacoma Creek watersheds. Prepared for Washington Department of Natural Resources, p. 61.

Laurel, D., & Wohl, E., 2019, The persistence of beaver-induced geomorphic heterogeneity and organic carbon stock in river corridors. Earth Surface Processes and Landforms, no. 1, p. 342-353.

Lewellen, D. G., Walker, C. W., and Cushman, C. D., 1985, Geology and coal potential of the Taneum-Manastash area. Kittitas County, Washington: Washington Division of Geology and Earth Resources Open-File Report, p. 83-9.

Lininger, K. B., Scamardo, J. E., & Guiney, M. R., 2021, Floodplain large wood and organic matter jam formation after a large flood: investigating the influence of floodplain forest stand characteristics and river corridor morphology. Journal of Geophysical Research: Earth Surface, no. 6, e2020JF006011.

Lininger, K. B., Wohl, E., Rose, J. R., & Leisz, S. J., 2019, Significant floodplain soil organic carbon storage along a large high-latitude river and its tributaries. Geophysical Research Letters, no. 4, p. 2121-2129.

May, C.L. and Gresswell, R.E., 2003, Large wood recruitment and redistribution in headwater streams in the southern Oregon Coast Range, USA. Canadian Journal of Forest Research, no. 8, p. 1352-1362.

Magilligan, F.J., Buraas, E.M. and Renshaw, C.E., 2015, The efficacy of stream power and flow duration on geomorphic responses to catastrophic flooding. Geomorphology, v. 228, p.175-188.

Martin, D.J., Pavlowsky, R.T., Bendix, J., Dogwiler, T. and Hess, J., 2021, Impacts of an extreme flood on large wood recruitment and transport processes. Physical Geography, p. 1-29.

McComb, W. C., Sedell, J. R., & Buchholz, T. D., 1990, Dam-site selection by beavers in an eastern Oregon basin. The Great Basin Naturalist, p. 273-281.

McKnight, P. E., & Najab, J, ,2010, Mann-Whitney U Test. The Corsini encyclopedia of psychology, p. 1-1.

Megahan, W.F., 1982, Channel sediment storage behind obstructions in forested drainage basins draining the granitic bedrock of the Idaho batholith. In: F.J. Swanson, R.J. Janda, T. Dunne, D.N. Swanston (Editors), Sediment Budgets and Routing in Forested Drainage Basins. USDA Forest Service Gen. Tech. Rep. PNW141, p. 114-121.

Monk, P.A., 2015, Steelhead Return to Taneum Creek Following Habitat Restoration. Prepared for U.S. Bureau of Reclamation, Yakima River Basin Water Enhancement Project, prepared by U.S. Fish and Wildlife Service, Mid-Columbia Fishery Resource

Monk, P., 2009, Taneum Creek Study: The Bruton-KRD Water Exchange Project. Bureau of Reclamation Open-File Report, p. 1-26.

Nagayama, S. and Nakamura, F., 2010, Fish habitat rehabilitation using wood in the world. Landscape and Ecological Engineering, no. 2, p. 289-305.

National Agriculture Imagery Program (NAIP), 2013, National Agriculture Imagery Program (NAIP) Information Sheet.

Osei, N.A., Gurnell, A.M. and Harvey, G.L., 2015, The role of large wood in retaining fine sediment, organic matter and plant propagules in a small, single-thread forest river. Geomorphology, vol. 235, p. 77-87.

R Core Team, 2020, R: A language and environment for statistical computing, R Foundation for Statistical Computing, Vienna, Austria, URL https://www.R-project.org/.

Roni, P., Beechie, T., Pess, G. and Hanson, K., 2015, Wood placement in river restoration: fact, fiction, and future direction. Canadian Journal of Fisheries and Aquatic Sciences, no. 3, p. 466-478.

Tabor, R. W.; Waitt, R. B., Jr.; Frizzell, V. A., Jr.; Swanson, D. A.; Byerly, G. R.; Bentley, R. D., 1982, Geologic map of the Wenatchee 1:100,000 quadrangle, central Washington: U.S. Geological Survey Miscellaneous Investigations Series Map I-1311, 1 sheet, scale 1:100,000, with 26 p. text. [http://pubs.er.usgs.gov/usgspubs/i/i1311/]

Tague, C., Valentine, S. and Kotchen, M., 2008, Effect of geomorphic channel restoration on streamflow and groundwater in a snowmelt-dominated watershed. Water resources research, no. 10, doi:10.1029/2007WR006418.

Tappel, P., 2011, Consideration of Large Wood Placed in Taneum Creek by the Yakima Indian Nation, with Respect to Flood Damages to Private Property in Mid-May 2011. Fisheries Engineers, Inc Open-File Report, p. 1-8.

Thompson, D.M. and Fixler, S.A., 2017, Formation and maintenance of a forced pool-riffle couplet following loading of large wood. Geomorphology, vol. 296, p.74-90.

Thompson, D. and Stull, G., 2002, The development and historic use of habitat structures in channel restoration in the United States: the grand experiment in fisheries management. Géographie physique et Quaternaire, no. 1, p. 45-60.

Toth, S, 1995, In Support of the Habitat Conservation Plan on Forested Lands Owned by Plum Creek Timber Company, L.P. in the I-90 Corridor of the Central Cascades Mountain Range, Washington, 1995. Technical Report #11

Saint-Laurent, D., Arsenault-Boucher, L., & Berthelot, J. S. 2019, Contrasting effects of flood disturbance on alluvial soils and riparian tree structure and species composition in mixed temperate forests. Air, Soil and Water Research, vol. 12.

Surian, N., Righini, M., Lucía, A., Nardi, L., Amponsah, W., Benvenuti, M., Borga, M., Cavalli, M., Comiti, F., Marchi, L. and Rinaldi, M., 2016, Channel response to extreme floods: insights on controlling factors from six mountain rivers in northern Apennines, Italy. Geomorphology, v. 272, p.78-91.

Swanson, F. J., Gregory, S. V., Iroumé, A., Ruiz-Villanueva, V., and Wohl, E., 2021, Reflections on the history of research on large wood in rivers. Earth Surface Processes and Landforms, no. 1, p. 55-66.

Vaccaro, J.J., Jones, M.A., Ely, D.M., Keys, M.E., Olsen, T.D., Welch, W.B., and Cox, S.E., 2009, Hydrogeologic framework of the Yakima River basin aquifer system, Washington: U.S. Geological Survey Scientific Investigations Report 2009–5152, 106 p.

Vaccaro, J.J., and Maloy, K.J., 2006, A thermal profile method to identify potential ground-water discharge areas and preferred salmonid habitats for long river reaches: U.S. Geological = Survey Scientific Investigations Report 2006-5136, 16 p.

Wigmore, O., Mark, B., McKenzie, J., Baraer, M., and Lautz, L., 2019, Sub-metre mapping of surface soil moisture in proglacial valleys of the tropical Andes using a multispectral unmanned aerial vehicle. Remote Sensing of Environment, v. 222, p. 104-118.

Wohl, E., 2013, Floodplains and wood. Earth-Science Reviews, v. 123, p. 194-212.

APPENDIXES

Appendix A – NDVI Data

Table A1: The Raw NDVI values for the Taneum Creek Reaches.

| Series | X | Y |
|---|---|---|
| Control Reach | 8/31/2006 | 0.27878 |
| Control Reach | 8/29/2007 | 0.268 |
| Control Reach | 8/15/2008 | 0.28526 |
| Control Reach | 8/2/2009 | 0.29094 |
| Control Reach | 8/5/2010 | 0.30725 |
| Control Reach | 8/24/2011 0:00 | 0.28707 |
| Control Reach | 8/10/2012 18:30 | 0.384296 |
| Control Reach | 8/13/2013 18:51 | 0.304875 |
| Control Reach | 8/7/2014 18:55 | 0.303308 |
| Control Reach | 8/19/2015 18:49 | 0.28476 |
| Control Reach | 8/21/2016 18:49 | 0.300992 |
| Control Reach | 8/8/2017 18:49 | 0.297381 |
| Control Reach | 8/18/2018 18:55 | 0.273762 |

| | | |
|---|---|---|
| Control Reach | 8/14/2019<br><br>18:49 | 0.320327 |
| Control Reach | 8/23/2020<br><br>18:55 | 0.29548 |
| Lower Reach | 8/31/2006 | 0.31355 |
| Lower Reach | 8/29/2007 | 0.3022 |
| Lower Reach | 8/15/2008 | 0.32679 |
| Lower Reach | 8/2/2009 | 0.32564 |
| Lower Reach | 8/5/2010 | 0.33987 |
| Lower Reach | 8/24/2011 0:00 | 0.34257 |
| Lower Reach | 8/10/2012<br><br>18:30 | 0.474656 |
| Lower Reach | 8/13/2013<br><br>18:51 | 0.356219 |
| Lower Reach | 8/7/2014 18:55 | 0.36713 |
| Lower Reach | 8/19/2015<br><br>18:49 | 0.330518 |
| Lower Reach | 8/21/2016<br><br>18:49 | 0.359619 |
| Lower Reach | 8/8/2017 18:49 | 0.358156 |
| Lower Reach | 8/18/2018<br><br>18:55 | 0.314613 |

| | | |
|---|---|---|
| Lower Reach | 8/14/2019<br><br>18:49 | 0.366184 |
| Lower Reach | 8/23/2020<br><br>18:55 | 0.361758 |
| Middle Reach | 8/31/2006 | 0.312 |
| Middle Reach | 8/29/2007 | 0.30741 |
| Middle Reach | 8/15/2008 | 0.33248 |
| Middle Reach | 8/2/2009 | 0.33234 |
| Middle Reach | 8/5/2010 | 0.34178 |
| Middle Reach | 8/24/2011 0:00 | 0.32897 |
| Middle Reach | 8/10/2012<br><br>18:30 | 0.495333 |
| Middle Reach | 8/13/2013<br><br>18:51 | 0.359181 |
| Middle Reach | 8/7/2014 18:55 | 0.364512 |
| Middle Reach | 8/19/2015<br><br>18:49 | 0.339327 |
| Middle Reach | 8/21/2016<br><br>18:49 | 0.354315 |
| Middle Reach | 8/8/2017 18:49 | 0.34337 |
| Middle Reach | 8/18/2018<br><br>18:55 | 0.308005 |

| | | |
|---|---|---|
| Middle Reach | 8/14/2019<br><br>18:49 | 0.37681 |
| Middle Reach | 8/23/2020<br><br>18:55 | 0.361012 |
| Upper Reach | 8/31/2006 | 0.31482 |
| Upper Reach | 8/29/2007 | 0.30945 |
| Upper Reach | 8/15/2008 | 0.33109 |
| Upper Reach | 8/2/2009 | 0.3317 |
| Upper Reach | 8/5/2010 | 0.3392 |
| Upper Reach | 8/24/2011 0:00 | 0.33267 |
| Upper Reach | 8/10/2012<br><br>18:30 | 0.472649 |
| Upper Reach | 8/13/2013<br><br>18:51 | 0.353822 |
| Upper Reach | 8/7/2014 18:55 | 0.348819 |
| Upper Reach | 8/19/2015<br><br>18:49 | 0.332618 |
| Upper Reach | 8/21/2016<br><br>18:49 | 0.33488 |
| Upper Reach | 8/8/2017 18:49 | 0.341223 |
| Upper Reach | 8/18/2018<br><br>18:55 | 0.302321 |

| | | |
|---|---|---|
| Upper Reach | 8/14/2019<br><br>18:49 | 0.363743 |
| Upper Reach | 8/23/2020<br><br>18:55 | 0.348918 |

Table A2: The raw data for the NDVI change from zero values.

| Reach | Date | Change from zero |
|---|---|---|
| Control Reach | 8/31/06 | 0 |
| Control Reach | 8/29/07 | -0.01078 |
| Control Reach | 8/15/08 | 0.00648 |
| Control Reach | 8/2/09 | 0.01216 |
| Control Reach | 8/5/10 | 0.02847 |
| Control Reach | 8/24/11 0:00 | 0.00829 |
| Control Reach | 8/10/12 18:30 | 0.105516 |
| Control Reach | 8/13/13 18:51 | 0.026095 |
| Control Reach | 8/7/14 18:55 | 0.024528 |
| Control Reach | 8/19/15 18:49 | 0.00598 |
| Control Reach | 8/21/16 18:49 | 0.022212 |
| Control Reach | 8/8/17 18:49 | 0.018601 |
| Control Reach | 8/18/18 18:55 | -0.00502 |
| Control Reach | 8/14/19 18:49 | 0.041547 |
| Control Reach | 8/23/20 18:55 | 0.0167 |
| Lower Reach | 8/31/06 | 0 |
| Lower Reach | 8/29/07 | -0.01135 |
| Lower Reach | 8/15/08 | 0.01324 |
| Lower Reach | 8/2/09 | 0.01209 |
| Lower Reach | 8/5/10 | 0.02632 |

| | | |
|---|---|---|
| Lower Reach | 8/24/11 0:00 | 0.02902 |
| Lower Reach | 8/10/12 18:30 | 0.161106 |
| Lower Reach | 8/13/13 18:51 | 0.042669 |
| Lower Reach | 8/7/14 18:55 | 0.05358 |
| Lower Reach | 8/19/15 18:49 | 0.016968 |
| Lower Reach | 8/21/16 18:49 | 0.046069 |
| Lower Reach | 8/8/17 18:49 | 0.044606 |
| Lower Reach | 8/18/18 18:55 | 0.001063 |
| Lower Reach | 8/14/19 18:49 | 0.052634 |
| Lower Reach | 8/23/20 18:55 | 0.048208 |
| Middle Reach | 8/31/06 | 0 |
| Middle Reach | 8/29/07 | -0.00459 |
| Middle Reach | 8/15/08 | 0.02048 |
| Middle Reach | 8/2/09 | 0.02034 |
| Middle Reach | 8/5/10 | 0.02978 |
| Middle Reach | 8/24/11 0:00 | 0.01697 |
| Middle Reach | 8/10/12 18:30 | 0.183333 |
| Middle Reach | 8/13/13 18:51 | 0.047181 |
| Middle Reach | 8/7/14 18:55 | 0.052512 |
| Middle Reach | 8/19/15 18:49 | 0.027327 |
| Middle Reach | 8/21/16 18:49 | 0.042315 |
| Middle Reach | 8/8/17 18:49 | 0.03137 |
| Middle Reach | 8/18/18 18:55 | -0.00399 |
| Middle Reach | 8/14/19 18:49 | 0.06481 |
| Middle Reach | 8/23/20 18:55 | 0.049012 |

| | | |
|---|---|---|
| Upper Reach | 8/31/06 | 0 |
| Upper Reach | 8/29/07 | -0.00537 |
| Upper Reach | 8/15/08 | 0.01627 |
| Upper Reach | 8/2/09 | 0.01688 |
| Upper Reach | 8/5/10 | 0.02438 |
| Upper Reach | 8/24/11 0:00 | 0.01785 |
| Upper Reach | 8/10/12 18:30 | 0.157829 |
| Upper Reach | 8/13/13 18:51 | 0.039002 |
| Upper Reach | 8/7/14 18:55 | 0.033999 |
| Upper Reach | 8/19/15 18:49 | 0.017798 |
| Upper Reach | 8/21/16 18:49 | 0.02006 |
| Upper Reach | 8/8/17 18:49 | 0.026403 |
| Upper Reach | 8/18/18 18:55 | -0.0125 |
| Upper Reach | 8/14/19 18:49 | 0.048923 |
| Upper Reach | 8/23/20 18:55 | 0.034098 |

Appendix B – Piezometer Data

Table B1: The Raw piezometer data for the lower, upper, and middle reaches.

| | Outside | | Inside | Groundwater movement | |
|---|---|---|---|---|---|
| Piezometer | Top to Bed | Water Height | Top to Bed | Water Height | |
| UPRP1 | 65.9 | 13.3 | 91.2 | 37.2 | -1.4 |
| UPRP2 | 65 | 18.5 | 90.8 | 43.9 | -0.4 |

| | | | | | |
|---|---|---|---|---|---|
| UPRP3 | 55.3 | 14.5 | 97.5 | 44.6 | -12.1 |
| UPRP4 | 57.9 | 39.5 | 97.3 | 54.4 | -24.5 |
| UPRP5 | 58.5 | 19.9 | 96.7 | 36.9 | -21.2 |
| UPRP6 | 55.6 | 27.2 | 96.3 | 52.9 | -15 |
| UPRP7 | 55.4 | 18.2 | 92.7 | 55.4 | -0.1 |
| UPRP8 | 68.8 | 24.2 | 88.1 | 45.2 | 1.7 |
| MRP0 TH | 81.3 | 27.6 | 93.1 | 39.8 | 0.4 |
| MRP1 TH | 73.3 | 17 | 92.9 | 34 | -2.6 |
| MRP2 TH | 55.5 | 24.7 | 92.8 | 42.7 | -19.3 |
| MRP3 TH | 73.1 | 51 | 95 | 63.7 | -9.2 |
| MRP4 TH | 83.1 | 62.9 | 88 | 69.6 | 1.8 |
| MRP4.5 RB | 81.2 | 52 | 85.8 | 60.4 | 3.8 |
| MRP5 TH | 86.4 | 60.7 | 88.7 | 62.5 | -0.5 |
| MRP6 RCTH | 82.9 | 6 | 96 | 19.9 | 0.8 |
| MRP6LCTH | 77.8 | 17.9 | 93.9 | 27.8 | -6.2 |
| MRP7RCTH | 79.3 | 7.5 | 87.4 | 13.1 | -2.5 |
| MRP7LCTH | 74.1 | 16.1 | 93.3 | 17.3 | -18 |
| MRP8RCTH | 79.7 | 11.3 | 92 | 23.2 | -0.4 |
| MRP8LCTH | 76.7 | 9.6 | 95.4 | 30.9 | 2.6 |
| MRP9TH | 64.6 | 14.2 | 89.8 | 20.2 | -19.2 |
| MRP10TH | 82.9 | 18.4 | 94.4 | 31.5 | 1.6 |
| MRP10.5TH | 81.5 | 45 | 91.5 | 55 | 0 |

| | | | | | |
|---|---|---|---|---|---|
| P1 | 78.5 | 16 | 89.6 | 28.1 | 1 |
| P2 | 81.5 | 42.3 | 88.9 | 49.6 | -0.1 |
| P3 | 82.4 | 16 | 92.8 | 27.1 | 0.7 |
| P4 | 74.3 | 18.5 | 90.3 | 35.9 | 1.4 |
| P5 | 69.9 | 11.2 | 88.5 | 29.9 | 0.1 |
| P6 | 80.4 | 26 | 92.5 | 37.2 | -0.9 |
| P6 | 64.7 | 34.5 | 89 | 60.6 | 1.8 |
| P7 | 79.2 | 40.2 | 87.4 | 51.4 | 3 |
| P8 | 81.7 | 27.9 | 91.2 | 41.4 | 4 |
| P9 | 79.4 | 26.3 | 91.5 | 37.6 | -0.8 |
| P10 | 73.9 | 17 | 91.1 | 33.5 | -0.7 |

Appendix C- Sinuosity and MTCI Data

Table C1: The raw data for the sinuosity values for the 4 study reaches.

| | | Sinuosity | | | | | Valley Length | | | |
|---|---|---|---|---|---|---|---|---|---|---|
| | | Lower | Middle | Upper | Control | | Lower | Middle | Upper | Control |
| | 7/16/2006 | 1.01 | 1.25 | 1.14 | 1.12 | | 1057 | 984 | 926 | 936 |
| | 7/1/2009 | 1.07 | 1.27 | 1.18 | 1.12 | | | | | |
| | 8/18/2011 | 1.11 | 1.29 | 1.15 | 1.12 | | | | | |
| | 8/18/2013 | 1.09 | 1.30 | 1.14 | 1.12 | | | | | |
| | 7/30/2015 | 1.13 | 1.26 | 1.18 | 1.13 | | | | | |
| | 10/9/2017 | 1.07 | 1.24 | 1.19 | 1.13 | | | | | |
| | 10/14/2019 | 1.07 | 1.24 | 1.21 | 1.13 | | | | | |

Table C2: The Raw MTCI values for all four reaches.

| Threaded Channel Index | | | | |
|---|---|---|---|---|
| | Control | Lower | Middle | Upper |
| 7/16/06 | 1.12 | 1.10 | 1.25 | 1.19 |
| 7/1/09 | 1.12 | 1.15 | 1.32 | 1.24 |
| 8/18/11 | 1.12 | 1.86 | 2.14 | 1.91 |
| 8/18/13 | 1.12 | 1.90 | 2.07 | 1.91 |
| 7/30/15 | 1.13 | 1.95 | 1.85 | 2.14 |
| 10/9/17 | 1.13 | 1.91 | 1.84 | 2.07 |
| 10/14/19 | 1.13 | 1.96 | 1.73 | 2.11 |

Table C3: The raw data for the salinity and temperature cross section at the middle reach.

| depth | salinity | temp_ | XS |
|---|---|---|---|
| 17.5 | 134.4 | 14 | 10 |
| 29 | 134.9 | 14 | 10 |
| 38.5 | 135.5 | 13.8 | 10 |
| 36 | 135.7 | 13.7 | 10 |
| 21.5 | 135.8 | 13.7 | 10 |
| 3 | 135.9 | 13.7 | 10 |
| 3 | 135.9 | 13.7 | 10 |
| 8 | 135.6 | 13.8 | 10 |
| 9.5 | 135.6 | 13.8 | 10 |
| 11.5 | 135.7 | 13.8 | 10 |

| | | | |
|---|---|---|---|
| 16 | 135.4 | 13.9 | 10 |
| 17 | 135.7 | 13.9 | 10 |
| 14.5 | 136.9 | 14.9 | 10 |
| 5 | 135.3 | 13.8 | 10 |
| 2 | 133.9 | 13.7 | 9 |
| 10.5 | 134.9 | 13.9 | 9 |
| 15 | 135.1 | 13.8 | 9 |
| 17.5 | 135 | 13.8 | 9 |
| 20 | 135.2 | 13.8 | 9 |
| 20 | 135.6 | 13.7 | 9 |
| 17.5 | 135.9 | 13.7 | 9 |
| 12 | 136 | 13.6 | 9 |
| 16 | 135.9 | 13.6 | 9 |
| 13.5 | 136.3 | 13.5 | 9 |
| 13.5 | 136.1 | 13.6 | 9 |
| 13 | 136.2 | 13.6 | 9 |
| 9 | 136.1 | 13.7 | 9 |
| 5.5 | 136.6 | 13.6 | 9 |
| 8 | 134.9 | 13.6 | 8 |
| 4 | 135.4 | 13.5 | 8 |
| 12 | 135.2 | 13.4 | 8 |
| 6 | 134.4 | 13.5 | 8 |
| 11.5 | 136 | 13.4 | 8 |

| | | | |
|---|---|---|---|
| 12 | 136.1 | 13.4 | 8 |
| 14.5 | 136.1 | 13.4 | 8 |
| 13 | 135 | 13.5 | 8 |
| 9.5 | 136.2 | 13.4 | 8 |
| 5 | 135.4 | 13.7 | 8 |
| 5 | 135.4 | 13.7 | 8 |
| 5.5 | 134.8 | 13.9 | 8 |
| 12 | 135.5 | 13.7 | 8 |
| 11 | 135.3 | 13.8 | 8 |
| 10 | 135.4 | 13.8 | 8 |
| 5 | 135.5 | 13.8 | 8 |
| 10 | 128.2 | 15.7 | 7 |
| 18.5 | 132.8 | 14.1 | 7 |
| 22 | 133.9 | 13.7 | 7 |
| 22 | 133.2 | 13.5 | 7 |
| 7.5 | 131.6 | 13.3 | 7 |
| 6 | 131.9 | 13.3 | 7 |
| 2 | 133.9 | 14.1 | 7 |
| 4 | 134.7 | 14 | 7 |
| 4 | 134.6 | 13.8 | 7 |
| 6 | 135 | 13.7 | 7 |
| 10 | 134.8 | 13.8 | 7 |
| 8.5 | 134.3 | 13.8 | 7 |

| | | | |
|---|---|---|---|
| 6.5 | 134.4 | 14 | 7 |
| 3 | 135.1 | 13.9 | 7 |
| 2 | 130.5 | 14.4 | 6 |
| 8 | 133.4 | 13.5 | 6 |
| 12.5 | 134.5 | 13.3 | 6 |
| 14 | 135 | 13.2 | 6 |
| 18 | 135.1 | 13.1 | 6 |
| 16 | 135.5 | 13.1 | 6 |
| 15.5 | 134.9 | 13.3 | 6 |
| 2 | 136.3 | 13.2 | 6 |
| 2 | 115.1 | 13.9 | 6 |
| 1 | 134.3 | 14.2 | 6 |
| 3 | 133.6 | 14 | 6 |
| 3 | 126.5 | 13.9 | 6 |
| 5 | 134.2 | 14 | 6 |
| 5 | 129 | 15.3 | 5 |
| 20 | 131.7 | 14.2 | 5 |
| 26 | 134.2 | 13.5 | 5 |
| 31 | 134.5 | 13.2 | 5 |
| 38 | 134.6 | 13.2 | 5 |
| 43 | 137.9 | 14.4 | 5 |
| 41 | 136.3 | 13.8 | 5 |
| 54 | 135.8 | 13.4 | 5 |

| | | | |
|---|---|---|---|
| 50.5 | 136.9 | 13.4 | 5 |
| 55 | 136.1 | 13.6 | 5 |
| 20 | 137.3 | 12.6 | 5 |
| 29 | 132.3 | 17.1 | 4 |
| 44 | 133.5 | 16.7 | 4 |
| 50 | 134.7 | 16.4 | 4 |
| 61 | 135.1 | 16.3 | 4 |
| 66 | 135.2 | 16.3 | 4 |
| 56 | 135 | 16.4 | 4 |
| 47 | 134.4 | 16.6 | 4 |
| 29 | 134.7 | 16.6 | 4 |
| 17 | 131.1 | 17.4 | 3 |
| 31 | 133.3 | 16.8 | 3 |
| 41 | 134 | 16.5 | 3 |
| 44 | 134.5 | 16.3 | 3 |
| 46 | 134.6 | 16.3 | 3 |
| 35 | 134.9 | 16.2 | 3 |
| 26 | 135.4 | 16.3 | 3 |
| 12 | 134.8 | 16.3 | 3 |
| 18 | 131.1 | 17.6 | 2 |
| 24 | 133 | 16.7 | 2 |
| 23 | 133.7 | 16.5 | 2 |
| 26 | 134.4 | 16.3 | 2 |

| | | | |
|---|---|---|---|
| 21 | 134.7 | 16.2 | 2 |
| 14 | 135 | 16.2 | 2 |
| 9 | 130.2 | 17.6 | 1 |
| 12 | 132.2 | 16.9 | 1 |
| 14 | 133 | 16.7 | 1 |
| 10 | 133.8 | 16.4 | 1 |
| 9 | 134.2 | 16.3 | 1 |
| 11 | 134.6 | 16.2 | 1 |
| 10 | 134.9 | 16.1 | 1 |
| 10 | 134.9 | 16.2 | 1 |
| 10 | 131.1 | 18.1 | 0 |
| 15 | 132.2 | 17.1 | 0 |
| 24 | 133.2 | 16.6 | 0 |
| 25 | 133.6 | 16.4 | 0 |
| 20 | 134.5 | 16.2 | 0 |
| 9 | 134.8 | 16.2 | 0 |

Appendix D – Salinity and Temperature Data

Table D1: The raw data for the salinity and temperature cross section at the Upper reach.

| Depth | salinity | temperature | XS |
|---|---|---|---|
| 36 | 134.6 | 14.3 | XS0 |
| 34 | 134.4 | 14.4 | XS0 |
| 28 | 134.2 | 14.5 | XS0 |
| 29 | 135.3 | 14.5 | XS0 |
| 26 | 134.6 | 14.7 | XS0 |
| 18 | 133.4 | 14.9 | XS0 |
| 15 | 132.1 | 15.3 | XS0 |
| 17 | 131.8 | 15.8 | XS0 |
| 20.5 | 129.6 | 16.3 | XS0 |
| 25 | 135 | 14.3 | XS0 |
| 31 | 134.5 | 14.6 | XS1 |
| 30 | 134 | 14.7 | XS1 |
| 30 | 133.6 | 14.8 | XS1 |
| 48 | 133.7 | 14.9 | XS1 |
| 53 | 132.8 | 15.1 | XS1 |
| 42 | 132.3 | 15.9 | XS1 |
| 18 | 127.7 | 17 | XS1 |
| 26 | 134.4 | 14.6 | XS1 |
| 7 | 135.3 | 10.7 | XS10 |

| | | | |
|---|---|---|---|
| 11.5 | 135 | 10.7 | XS10 |
| 20 | 134.9 | 10.7 | XS10 |
| 33 | 135.3 | 10.6 | XS10 |
| 35 | 133.5 | 10.6 | XS10 |
| 38 | 135.2 | 10.6 | XS10 |
| 50 | 135 | 10.5 | XS10 |
| 36 | 135.6 | 10.5 | XS10 |
| 33 | 134.1 | 14.9 | XS2 |
| 25.5 | 133.7 | 15 | XS2 |
| 19 | 133.8 | 15 | XS2 |
| 17.5 | 133.3 | 15.1 | XS2 |
| 21.5 | 133.4 | 15.1 | XS2 |
| 27 | 133.2 | 15.4 | XS2 |
| 20 | 131 | 16.1 | XS2 |
| 8 | 129.6 | 16.8 | XS2 |
| 28 | 134.4 | 14.9 | XS2 |
| 5 | 148.6 | 16.3 | XS3 |
| 25 | 133 | 15.3 | XS3 |
| 8 | 135.3 | 15.4 | XS3 |
| 6 | 135.2 | 15.6 | XS3 |
| 2 | 138.4 | 15.8 | XS3 |
| 30 | 133.3 | 15.3 | XS3 |
| 1 | 64.3 | 20.2 | XS4 |

| | | | |
|---|---|---|---|
| 24 | 131.8 | 16 | XS4 |
| 20 | 127.6 | 16.3 | XS4 |
| 13.5 | 109.5 | 17.6 | XS4 |
| 25 | 132.4 | 15 | XS4 |
| 30 | 125.3 | 18.2 | XS5 |
| 32 | 130.3 | 16.5 | XS5 |
| 18 | 132 | 16.1 | XS5 |
| 10 | 131.2 | 16 | XS5 |
| 12 | 132.5 | 16 | XS5 |
| 8 | 133.1 | 15.8 | XS5 |
| 5.5 | 133.1 | 15.8 | XS5 |
| 7 | 123 | 14.3 | XS6 |
| 10 | 128.3 | 12.8 | XS6 |
| 14 | 130.7 | 12 | XS6 |
| 8 | 131.7 | 11.6 | XS6 |
| 6 | 132.5 | 11.3 | XS6 |
| 10 | 133.4 | 11.1 | XS6 |
| 5 | 132.2 | 11.3 | XS6 |
| 4 | 124.6 | 13.7 | XS7 |
| 9 | 134.2 | 11 | XS7 |
| 15 | 130.8 | 11.1 | XS7 |
| 11 | 133 | 11.2 | XS7 |
| 8 | 127 | 11.7 | XS7 |

| | | | |
|---|---|---|---|
| 9 | 130.8 | 11.9 | XS7 |
| 2 | 129.7 | 12.5 | XS7 |
| 19 | 132.8 | 11.4 | XS7 |
| 10 | 133.5 | 11.1 | XS7 |
| 10 | 129.9 | 12.2 | XS8 |
| 30 | 134.1 | 10.8 | XS8 |
| 70 | 134.5 | 10.8 | XS8 |
| 68 | 134.2 | 10.9 | XS8 |
| 63 | 133.7 | 11.2 | XS8 |
| 50 | 132.2 | 11.6 | XS8 |
| 20.5 | 134.9 | 10.7 | XS8 |
| 21 | 132.1 | 11.6 | XS9 |
| 31 | 133 | 11.8 | XS9 |
| 29 | 133.8 | 11 | XS9 |
| 45 | 134.6 | 10.9 | XS9 |
| 61 | 134.9 | 10.8 | XS9 |
| 70 | 134.9 | 10.7 | XS9 |
| 68 | 135.3 | 10.6 | XS9 |
| 50 | 135.1 | 10.6 | |
| 7 | 132.7 | 16.3 | |
| 14.5 | 131.4 | 16.1 | |

Appendix E – Maps


Figure E1: The MTCI for the upper reach.

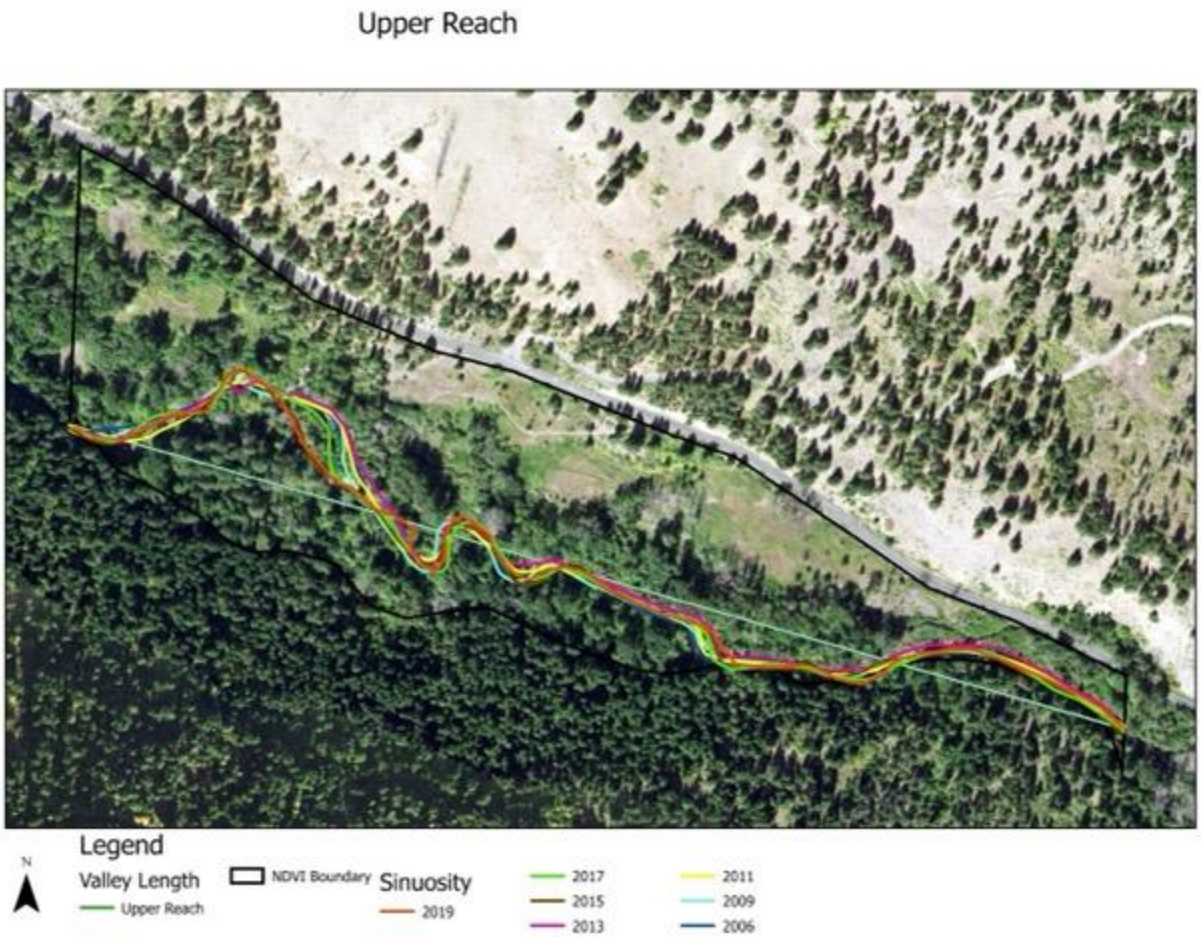

Figure E2: The sinuosity for the upper reach.

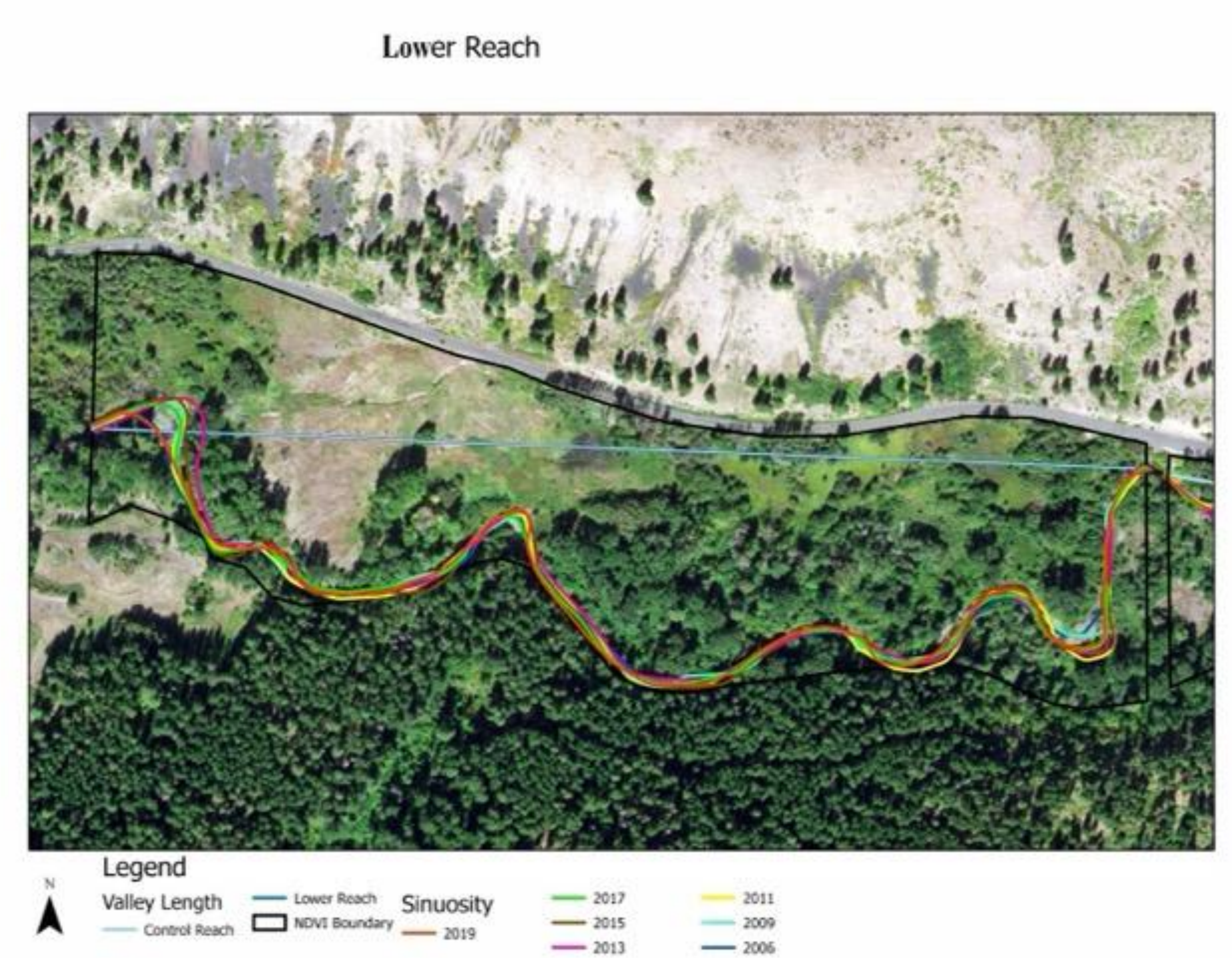


Figure E3: The sinuosity for the lower reach.

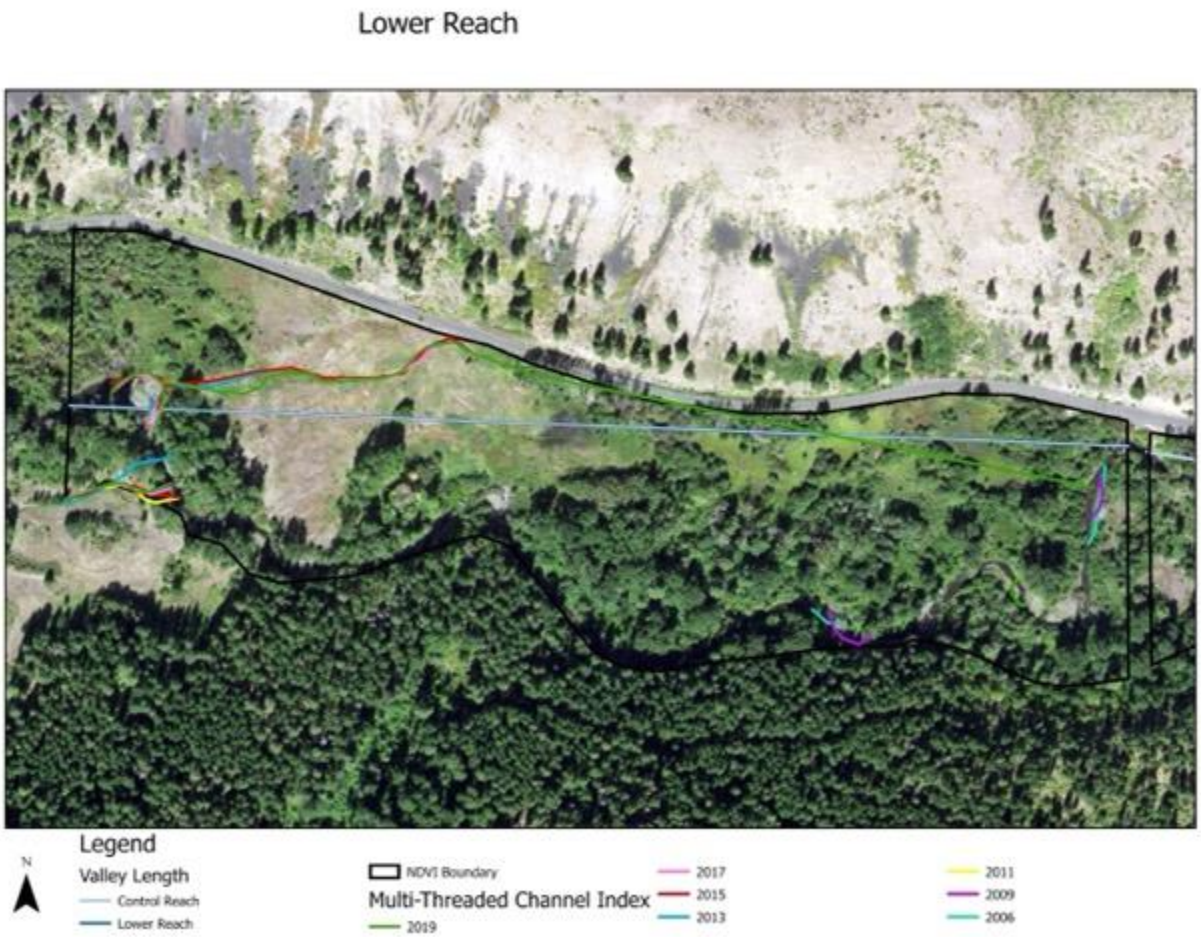

Figure E4: The MTCI for the lower reach.

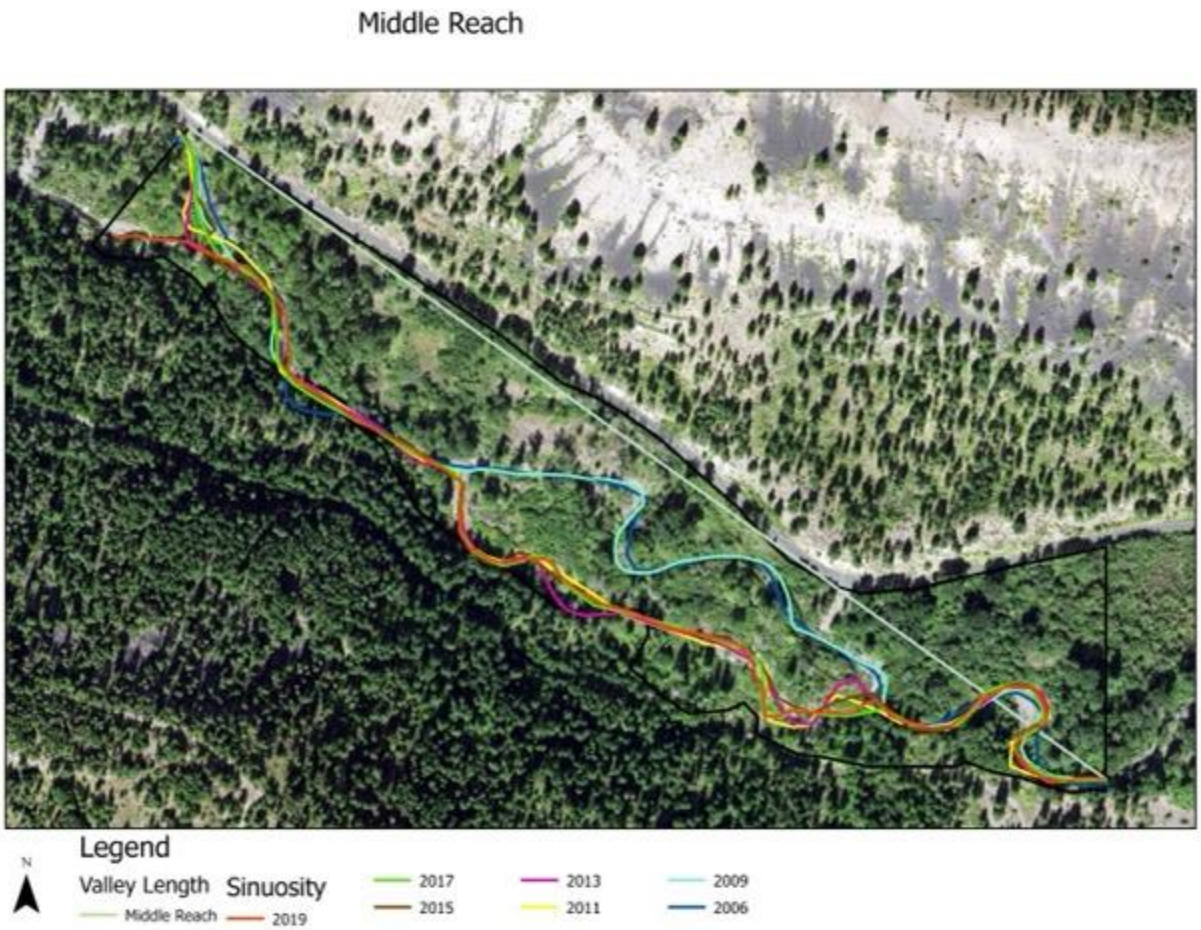

Figure E5: The sinuosity for the middle reach.

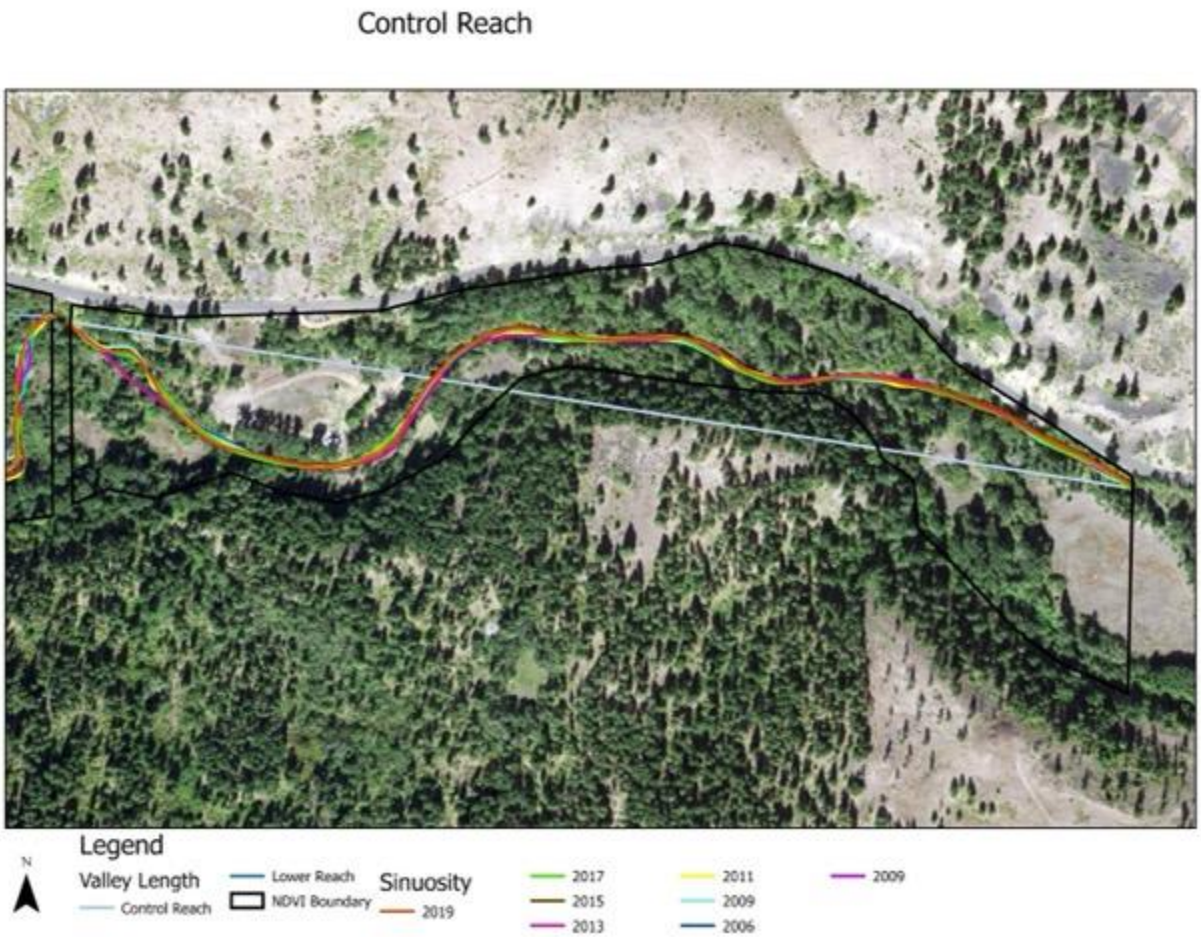

Figure E6: The sinuosity for the control reach.

Appendix F - Drone Imagery

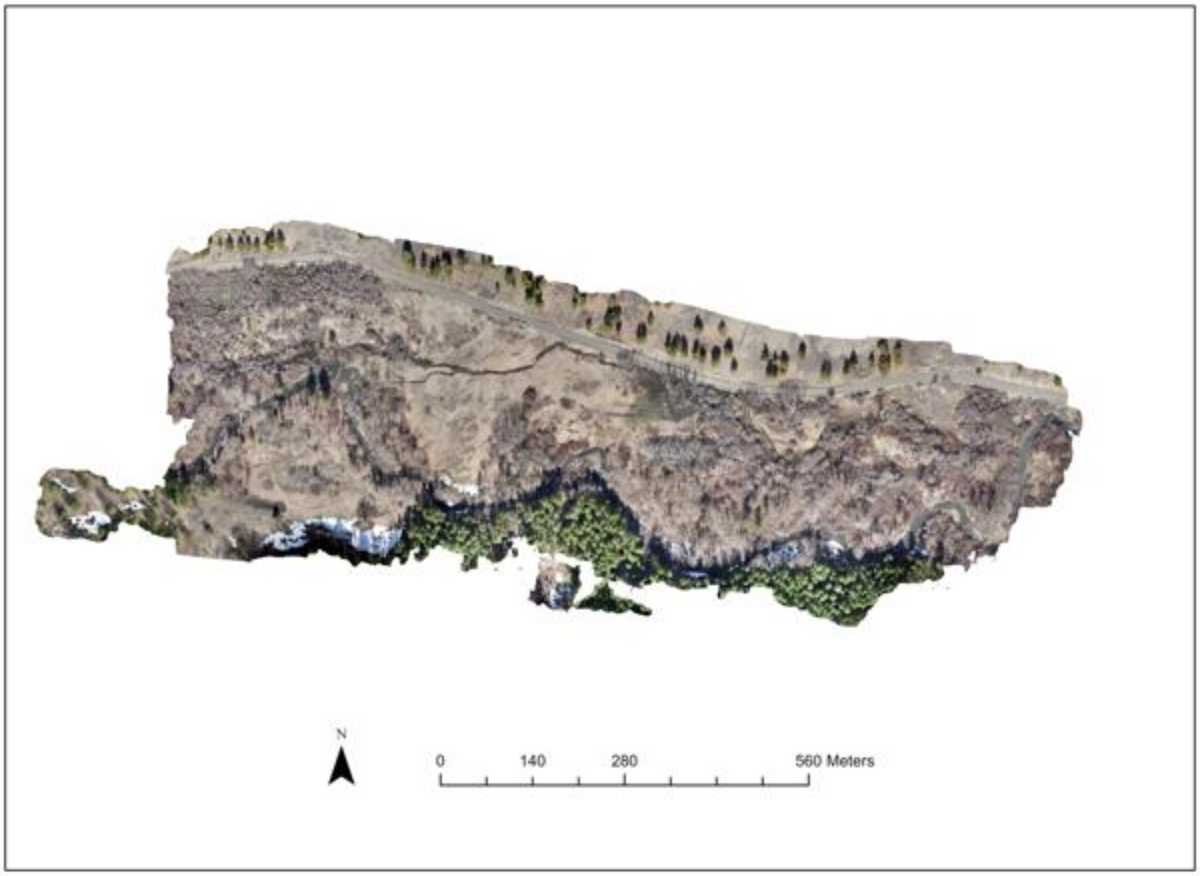


Figure F1: Drone imagery for the lower reach, spring 2021.


Figure F2: Drone imagery for the lower reach, spring 2022.

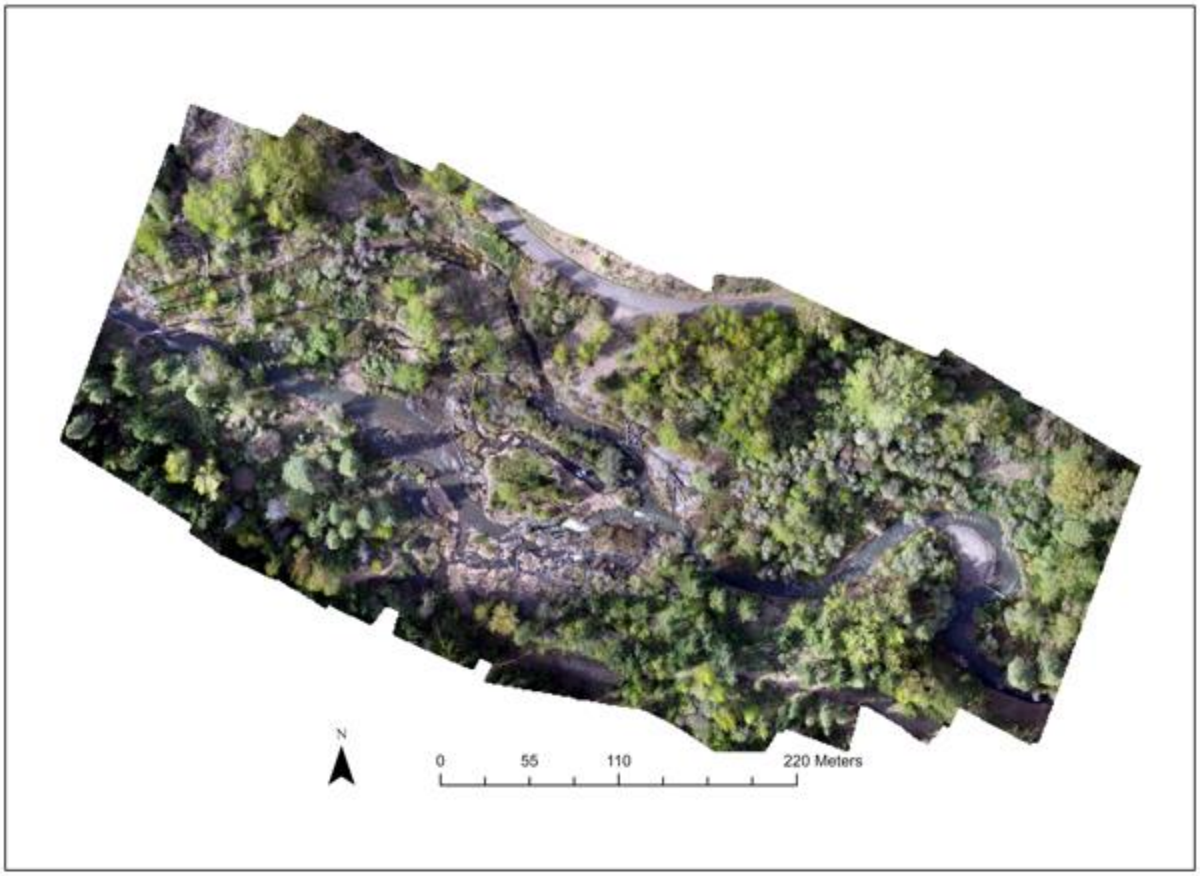


Figure F3: Drone imagery for the middle reach, spring 2021.

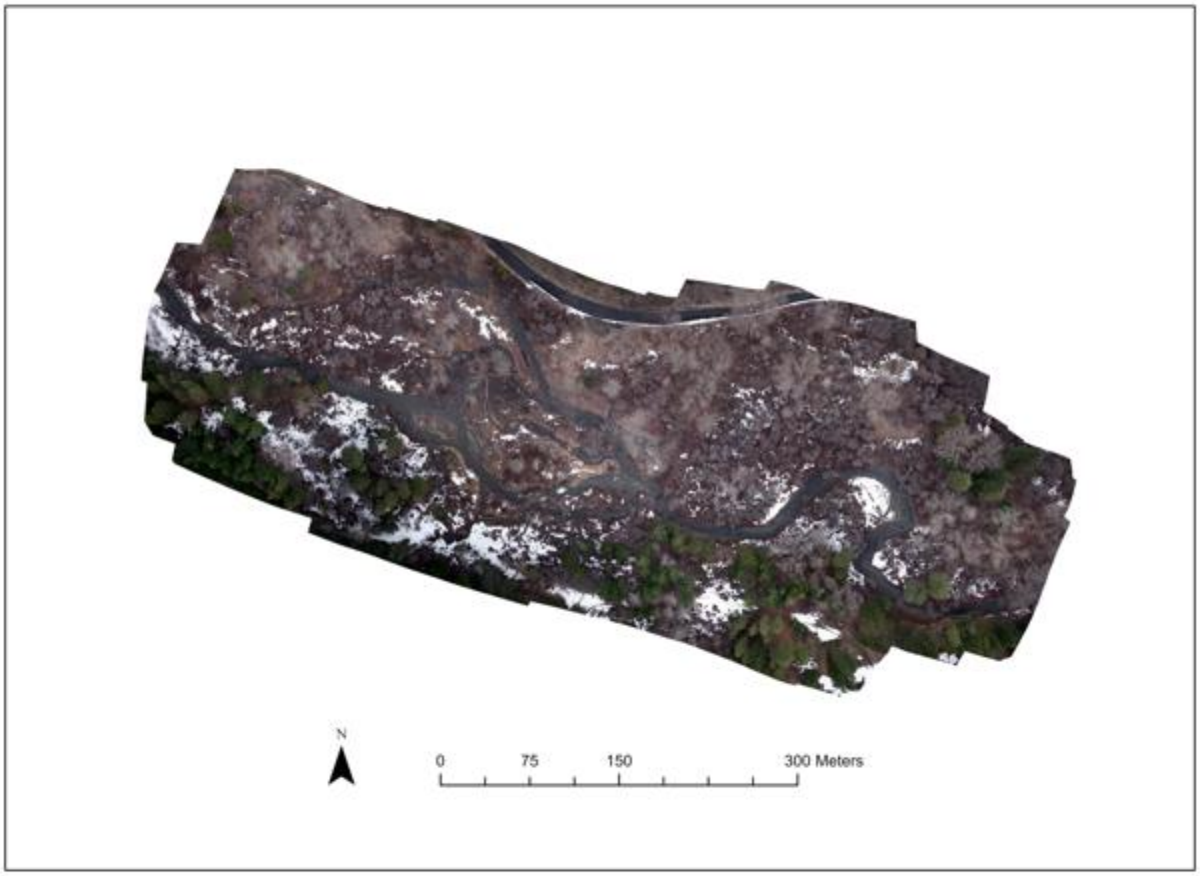


Figure F4: Drone imagery for the middle reach, spring 2022.

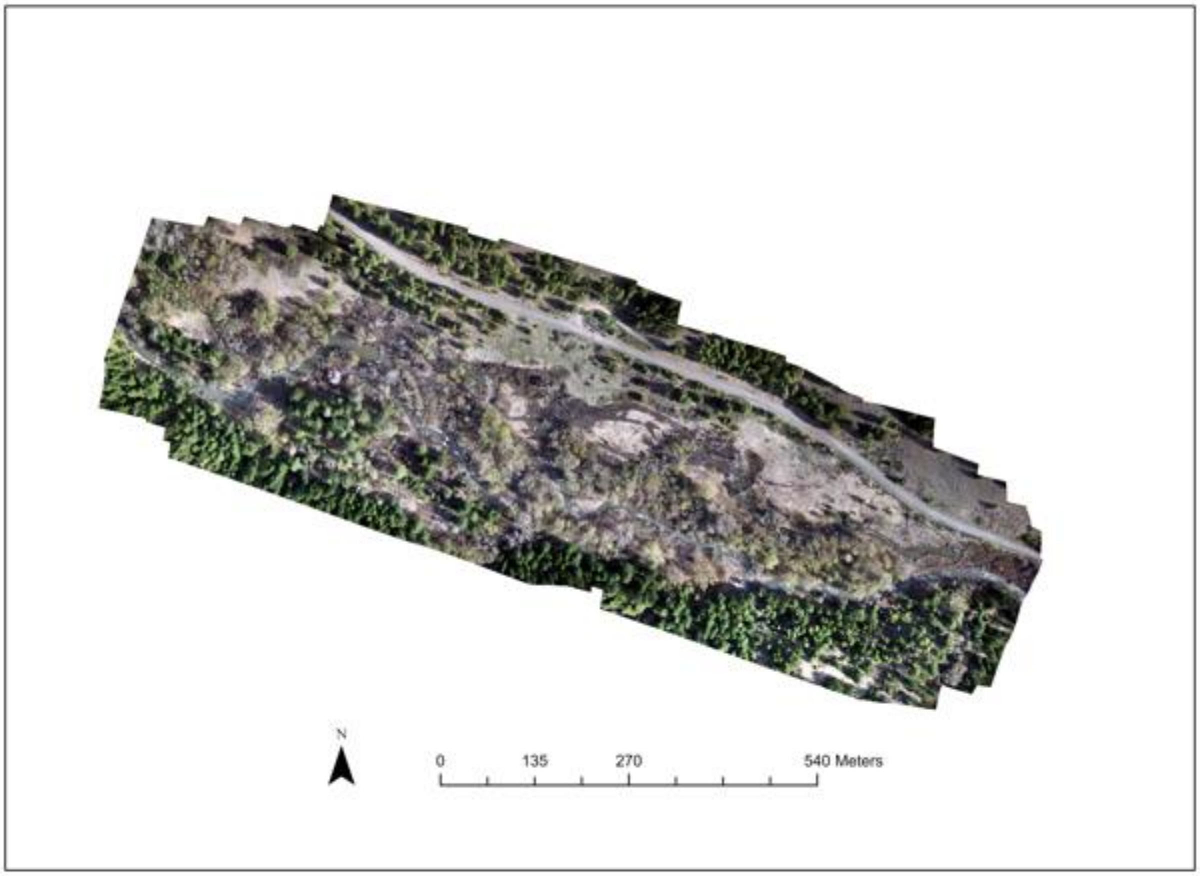


Figure F5: Drone imagery for the upper reach, spring 2021.